CGRP inhibits human Langerhans cells infection with HSV by differentially modulating specific HSV-1 and HSV-2 entry mechanisms

Emmanuel Cohen, Jammy Mariotton, Flore Rozenberg, Anette Sams, Toin van Kuppevelt, Nicolas Barry Delongchamps, Marc Zerbib, Morgane Bomsel, Yonatan Ganor

CGRP inhibits human Langerhans cells infection with HSV by differentially modulating specific HSV-1 and HSV-2 entry mechanisms

Emmanuel Cohen[1], Jammy Mariotton[1], Flore Rozenberg[2], Anette Sams[3], Toin H. van Kuppevelt[4], Nicolas Barry Delongchamps[5], Marc Zerbib[5], Morgane Bomsel[1], Yonatan Ganor[1,*]

[1]Laboratory of Mucosal Entry of HIV-1 and Mucosal Immunity, Cochin Institute, Université de Paris, INSERM U1016, CNRS UMR8104, Paris, France; [2]Virology Service, Cochin Hospital, Paris, France; [3]Department of Clinical Experimental Research, Glostrup Research Institute, Glostrup Hospital, Rigshospitalet, Denmark; [4]Department of Biochemistry, Radboud Institute for Molecular Life Sciences, Radboud university medical center, Nijmegen, The Netherlands; [5]Urology Service, GH Cochin-St Vincent de Paul, Paris, France.

[*]**Corresponding author**: Yonatan Ganor

Email: yonatan.ganor@inserm.fr

Tel: +33-1-40-51-64-45

Abstract

Herpes simplex virus (HSV) is widespread globally, with both HSV-1 and HSV-2 responsible for genital herpes. During sexual transmission, HSV targets epithelial cells, sensory peripheral pain neurons secreting the mucosal neuropeptide calcitonin gene-related peptide (CGRP), and mucosal immune cells including Langerhans cells (LCs). We previously described a neuro-immune crosstalk, whereby CGRP inhibits LCs-mediated human immunodeficiency virus type 1 (HIV-1) transmission. Herein, to further explore CGRP-mediated anti-viral function, we investigated whether CGRP affects LCs infection with HSV.

We found that both HSV-1 and HSV-2 primary isolates productively infect monocyte-derived LCs (MDLCs) and inner foreskin LCs. Moreover, CGRP significantly inhibits infection with both HSV subtypes of MDLCs and langerin^{high}, but not langerin^{low}, inner foreskin LCs. For HSV-1, infection is mediated via the HSV-1-specific entry receptor 3-O sulfated heparan sulfate (3-OS HS) in a pH-depended manner, and CGRP down-regulates 3-OS HS surface expression, as well as abrogates pH dependency. For HSV-2, infection involves langerin-mediated endocytosis in a pH-independent manner, and CGRP up-regulates surface expression of atypical langerin double-trimer oligomers.

Our results show that CGRP inhibits mucosal HSV infection by differentially modulating subtype-specific entry receptors and mechanisms in human LCs. CGRP could turn out useful for prevention of LCs-mediated HSV infection and HSV/HIV-1 co-infection.

Introduction

According to the World Health Organization, in 2016 around 3.7 and 0.5 billion people under the age of 50 (i.e. 67% and 13% of the world's population) were infected with herpes simplex virus (HSV)-1 and HSV-2, respectively, making HSV a highly prevalent sexually transmitted infection (STI) [1]. HSV-1 induces painful orofacial herpes, as well as life threatening meningitis, keratitis, encephalitis and neonatal infection [2]. Both HSV-2 and HSV-1 induce genital ulcers [3, 4], and HSV-2 is the largest STI contributor and risk factor for increased HIV-1 acquisition during co-infection [5].

HSV sexual transmission occurs once the virus invades the protective mucosal barriers of genital epithelia and targets epithelial cells (i.e. epitheliotropic) in a lytic cycle [6]. Subsequently, HSV enters the nerve endings of sensory peripheral neurons (i.e. neurotropic), in which it establishes life-long latency. Episodes of recurrence occur when latent HSV is reactivated and transported back by anterograde axonal transport close to the initial site of infection [6]. HSV-1 establishes latency in a subset of sensory peripheral pain neurons termed nociceptors that secret the mucosal vasodilator neuropeptide calcitonin gene-related peptide (CGRP) [7]. Such latency is established both in human [8] and murine [9] $CGRP^+$ nociceptors, in which latent HSV-1 decreases CGRP secretion [10]. In contrast, HSV-2 establishes latency in a different population of $CGRP^{low}$ murine nociceptors [11].

Different types of resident immune cells within genital epithelia are also HSV and HIV-1 cellular targets, including antigen-presenting Langerhans cells (LCs). Indeed, LCs can be productively infected with HSV, leading to their apoptosis and transfer of HSV antigens to dermal dendritic cells (DCs), facilitating viral relay (reviewed in [12]). Previous studies (included our own) also demonstrated infection of LCs with HIV-1, e.g. at high HIV-1 doses or following cell activation [13-18], followed by transfer of intact infectious HIV-1 virions from LCs to $CD4^+$ T-cells in a temporal manner [19, 20]. During co-infection, HSV-2 competes with HIV-1 for binding to the LC-specific C-type lectin langerin, thereby decreasing langerin availability and langerin-mediated HIV-1 degradation [21]. HSV-

2 also increases expression of the HIV-1 receptor CD4 and co-receptor CCR5 in LCs, thereby enhancing their susceptibility to HIV-1 infection [22, 23].

Recent studies provide evidence for the complexity of the LC network within the epithelial compartment, by describing several cell subsets that can be distinguished by their expression levels of CD1a and langerin. These studies identified CD1a^{high}langerin^{high} LCs, termed LC1 by one study, in the epidermis of the inner foreskin and skin [24, 25]. Additional CD1a^{low}langerin$^{neg/low}$ cells were also identified, and combined with differential expression of CD11c or CD1c, were termed epidermal dendritic cells (Epi-cDC2s) [24] or LC2 [25], respectively. As a proportion of Epi-cDC2s expresses langerin in the inner foreskin (but only a very low proportion expresses langerin in skin), coinciding with the high frequency of the LC2 subset in inner foreskin, it remains to be determined whether langerin-expressing Epi-cDC2s and LC2 represent the same or distinct LC subsets.

Sensing of and protecting from invading pathogens is orchestrated by a local mucosal neuro-immune crosstalk between immune cells and nociceptors, mediated via direct contacts and nociceptor-secreted neuropeptides, including CGRP [26]. This 37 amino acid neuropeptide is a potent vasodilator that plays important physiological and pathophysiological roles [7], and can directly modulate immune function in a vasodilator-independent manner. For instance, nociceptors associate with LCs and CGRP shifts LCs-mediated antigen presentation and cytokine secretion from Th1 to Th2/Th17 [27]. We previously discovered that CGRP also exerts anti-viral activity, as it strongly inhibits LCs-mediated HIV-1 transfer to CD4$^+$ T-cells via a multitude of co-operative mechanisms [19, 28, 29]. Accordingly, CGRP increases langerin surface expression and facilitates efficient viral degradation, by diverting HIV-1 from endo-lysosomes towards faster viral proteasomal degradation. CGRP also decreases LCs expression of adhesion molecules, leading to reduced formation of conjugates with CD4$^+$ T-cells, to limit viral transfer.

Herein, to further explore the extent of CGRP-mediated anti-viral function, we investigated whether CGRP could affect infection of LCs with HSV. Our results show that CGRP significantly inhibits

human LCs infection with both HSV-1 and HSV-2, via distinct effects that are related to modification of subtype-specific HSV entry receptors and mechanisms.

Results

Human LCs express HSV-1 and HSV-2 entry receptors

HSV uses several cell surface receptors to mediate its cellular entry (reviewed in [30]). Some of these receptors are subtype-specific, namely paired-immunoglobulin-like receptor alpha (PILR-α) is specific to HSV-1, while nectin-2 is specific to HSV-2. In contrast, nectin-1 and herpes-virus entry mediator (HVEM) are not subtype-specific and can be used by both HSV-1 and HSV-2. In addition, heparan sulfate (HS) proteoglycans are attachment receptors for both HSV-1 and HSV-2, yet the 3-O sulfated form of HS (3-OS HS) serves as an HSV-1-specific fusion receptor.

To test for expression of HSV receptors, human monocytes (i.e. LC precursors under inflammatory conditions) and monocyte-derived LCs (MDLCs) were surface labeled using specific antibodies (Abs) directed against the abovementioned HSV entry receptors and langerin, and analyzed by flow cytometry. As shown in Figure 1, monocytes expressed negligible levels of nectin-1, nectin-2 and 3-OS HS, while approximately 15% expressed HVEM and 45% expressed PILR-α (Figure 1A). Differentiation of monocytes into MDLCs resulted, as expected, in high CD1a and loss of CD14 expression in >95% of MDLCs, as well as expression of langerin in approximately 30% of MDLCs (Supplementary Figure 1A). Monocytes-to-MDLCs differentiation also reduced PILR-α, but increased HVEM and induced nectin-1, nectin-2 and 3-OS HS expression on ≥90% MDLCs (Figure 1B and Supplementary Figure 2).

We next confirmed the presence of CD1a^{high}langerin^{high} and CD1a^{low}langerin^{low} LC subsets within langerin^{+} inner foreskin epidermal cells, we termed herein langerin^{high} or langerin^{low} cells (Supplementary Figure 1B). Of note, based on their expression of high and uniform CD1a levels, MDLCs cannot be separated into similar subsets and were therefore gated, below and in ensuing experiments, on all langerin^{+} MDLCs (Supplementary Figure 1A). Compared to MDLCs, inner foreskin langerin^{+} cells (i.e. including langerin^{high} and langerin^{low} cells together) expressed all HSV

entry receptors tested, but at lower levels (Figure 1C). While langerin^{high} and langerin^{low} cells expressed similar levels of HVEM, PILR-α and 3-OS HS, langerin^{high} cells expressed higher nectin-1 and lower nectin-2 (Supplementary Figure 2).

These results indicate that human LCs might be permissive to infection with both HSV-1 and HSV-2.

Human LCs are productively infected with both HSV-1 and HSV-2

To evaluate HSV infection of human LCs, we pulsed MDLCs for 2hr with primary isolates of either HSV-1 or HSV-2. The cells were next washed with low pH buffer in order to remove surface-bound virions, stained for surface langerin and intracellular HSV-1/2-gD (i.e. an HSV-1/2 envelope glycoprotein that is a late gene product, whose expression is indicative of productive infection), and examined by flow cytometry.

These experiments showed that while MDLCs were not infected immediately following the 2hr viral pulse period (Figure 2A), a double langerin^{+}HSV-1/2-gD^{+} population could be observed 24hr post-infection (pi) with both HSV subtypes (Figure 2B). As expected, using primary isolates of HSV, infection was isolate-dependent, i.e. different primary isolates used at either low or high multiplicities of infection (MOIs) induced varying degrees of infection (Figure 2C), calculated as the percentage of langerin^{+}HSV-1/2-gD^{+} cells out of total langerin^{+} MDLCs (broken line frames in Figure 2B). In addition, both HSV-1 and HSV-2 infection of MDLCs was time-dependent (Figure 2D).

To demonstrate that MDLCs infection was productive, we collected their culture supernatants and measured the amounts of secreted infectious virus by standard plaque assay using HSV-permissive Vero cells. These experiments showed that MDLCs released infectious HSV-1 and HSV-2 at 24hr pi, at levels that correlated with that measured by HSV-1/2-gD intracellular staining (Figure 2E).

Finally, we evaluated HSV-induced apoptosis of human LCs by flow cytometry. These experiments showed that the proportion of apoptotic MDLCs (i.e. defined as langerin^{+} Annexin^{+} Propidium Iodide (PI)$^{-}$ cells) increased over time following HSV infection, and was significantly higher for both HSV

subtypes only at 72hr pi, compared to non-infected MDLCs (Figure 2F). At these different time points, cell viability of both non-infected and HSV-infected langerin^{+} MDLCs was of approximately 90% (Supplementary Figure 3). Therefore, in subsequent experiments using MDLCs, HSV infection was measured at 24-48hr pi to ensure the absence of notable apoptosis.

To further extend the findings obtained with MDLCs, we pulsed inner foreskin epidermal cell suspensions for 24hr with primary isolates of either HSV-1 or HSV-2, and evaluated infection at 48hr pi by flow cytometry as above. These experiments showed that langerin^{high} and langerin^{low} cells (see the gating strategy in Supplementary Figure 1B) could be infected with both HSV-1 and HSV-2 (Figure 3A). We next calculated infection separately for langerin^{high} and langerin^{low} cells, as the percentages of langerin^{high}HSV-1/2-gD^{+} out of total langerin^{high} (broken line frames in Figure 3A) or langerin^{low}HSV-1/2-gD^{+} out of total langerin^{low} cells (solid line frames in Figure 3A). This analysis showed that HSV-1 infection of langerin^{high} cells did not significantly differ from that of langerin^{low} cells (Figure 3B), with mean±SEM (derived from n=6 independent experiments using different inner foreskin tissues) infection percentages of 9.9±3.4 vs. 10.4±2.2. In contrast, HSV-2 infection of langerin^{high} cells was significantly higher than that of langerin^{low} cells (6.3±1.4 vs. 4.5±1.2, p=0.0023, paired Student's t-test), suggestive of langerin usage by HSV-2.

These results demonstrate that human LCs are productively infected with both HSV-1 and HSV-2.

CGRP inhibits human LCs infection with both HSV-1 and HSV-2

To investigate the potential impact of CGRP on HSV infection, MDLCs were left untreated or pre-treated for 24hr with different molar concentration of CGRP, within its effective concentration range that significantly inhibits MDLCs-mediated HIV-1 transfer to CD4^{+} T-cells, as we previously showed [29]. MDLCs were also pre-treated with SAX, a metabolically stable analogue of CGRP, which also inhibits MDLCs-mediated HIV-1 transfer, as we recently reported [31]. The cells were then pulsed with primary isolates of HSV-1 or HSV-2 for 2hr and infection was examined 24-48hr pi by flow

cytometry as above. To account for variations related to the use of MDLCs from different donors that were infected with different HSV-1/2 primary isolates at different MOIs (as shown in Figure 1C), infection was normalized to that of untreated cells serving as the 100% set point and averaged.

These experiments showed that CGRP and SAX dose-dependently inhibited MDLCs infection at 24hr pi, with both HSV-1 and HSV-2 (Figure 4A, B; see Supplementary Figure 4 for the separate non-normalized dose-responses curves). For both HSV subtypes, SAX-mediated inhibition was more potent than that of CGRP, with respective pIC_{50} potencies [95% confidence intervals] values of 9.5 [10.5-8.8] vs. 7.5 [9.2-5.1] for HSV-1, and 7.1 [8.7-5.4] vs. 5.8 [7.2-2.3] for HSV-2. In addition, CGRP-mediated inhibition was time-dependent, reaching 70-75% inhibition at 48hr pi for both HSV-1 and HSV-2 (Figure 4C). Importantly, CGRP also significantly inhibited the release of infectious HSV-1 and HSV-2 at 24hr pi (Figure 4D). Of note, as only a proportion of MDLCs expresses langerin (Supplementary Figure 1) that is increased following CGRP pre-treatment (as we previously reported [29] and confirmed below), the inhibitory effect of CGRP on HSV-1 and HSV-2 infection of MDLCs might be attributed to increased percentages of langerin$^+$ MDLCs. Yet, CGRP pre-treatment resulted in decreased percentages of langerin$^+$HSV-1/2-gD$^+$ double positive cells (data not shown), indicating actual inhibition of MDLCs infection.

We next used inner foreskin epidermal cell suspensions, which were left untreated or pre-treated for 24hr with CGRP. The cells were then pulsed with primary isolates of HSV-1 or HSV-2 for 24hr, and infection was examined 48h pi by flow cytometry. As for MDLCs, infection was normalized to that of untreated cells, in order to account for variations related to the use of tissues from different donors (as shown in Figure 3B). These experiments showed that following CGRP pre-treatment, infection was significantly decreased for both HSV subtypes in langerin^{high} cells (Figure 4E). In contrast, CGRP had no effect on infection of langerin^{low} cells with either HSV-1 or HSV-2 (Figure 4F).

These results demonstrate that CGRP exerts anti-viral activities during human LCs infection with both HSV-1 and HSV-2, and inhibits infection of MDLCs and langerin^{high}, but not langerin^{low}, inner foreskin LCs.

CGRP inhibits 3-OS HS-dependent and pH-dependent HSV-1 infection of human LCs

We next used MDLCs in order to characterize HSV-1 receptor usage, entry mechanism and CGRP-mediated inhibition. To determine which receptors mediate HSV-1 infection, we first pre-incubated HSV-permissive Vero cells for 1hr at 37°C with neutralizing Abs (nAbs) to HSV-1 entry receptors (i.e. nectin-1, HVEM and PILR-α) and confirmed by plaque assay their capacity to inhibit infection with HSV-1 primary isolates (Supplementary Figure 5). We then pre-incubated untreated and CGRP-treated MDLCs with the HSV-1 entry receptor nAbs, as well as with a langerin nAb (i.e. as one recent study reported langerin usage by HSV-1 in abdominal skin LCs [32]). MDLCs were also pre-incubated with heparinase, which cleaves HS / 3-OS HS [33], as we confirmed herein (Supplementary Figure 6). The cells were next pulsed for 2hr with HSV-1 primary isolates and infection was measured 24hr pi by flow cytometry. These experiments showed that none of the nAbs could significantly block HSV-1 infection of untreated MDLCs (Figure 5A). In contrast, pre-treatment with heparinase strongly inhibited HSV-1 infection (Figure 5A). Importantly, heparinase decreased by almost 80% not only the set-up infection of untreated cells, but also the reduced infection of CGRP-treated cells (Figure 5B). We next tested the effect of CGRP on 3-OS HS expression and found that CGRP significantly decreased the mean fluorescent intensity (MFI) of 3-OS HS surface expression in MDLCs (Figure 5C). In contrast, CGRP treatment had no effect on expression of other HSV-1/2 entry receptors (Supplementary Figure 7).

To further extend these observations, we pre-incubated untreated and CGRP-treated inner foreskin epidermal cell suspensions with heparinase or the langerin nAb, followed by 24h pulse with primary isolates of HSV-1 and evaluation of infection at 48h pi by flow cytometry. Focusing on langerin^{high}

cells, in which CGRP inhibits HSV-1 infection (see Figure 4E), these experiments showed that heparinase significantly decreased HSV-1 infection in both untreated and CGRP-treated langerin^{high} cells (Figure 5D). In contrast to MDLCs, the langerin nAb could inhibit HSV-1 infection in langerin^{high} cells (Figure 5D). CGRP also decreased 3-OS HS surface expression in langerin^{high} cells, with mean±SEM percentages of 3-OS HS-positive cells of 10.2±1.5 vs. 6.2±0.8 (as evaluated in epidermal suspensions of two individuals).

These results show that HSV-1 uses 3-OS HS to enter untreated and CGRP-treated MDLCs, and both 3-OS HS and langerin in inner foreskin langerin^{high} LCs.

Following receptor binding, HSV-1/2 entry is mediated by pH-independent fusion with the plasma membrane, and/or endocytic fusion that can be pH-independent or low pH-dependent [34]. We therefore pulsed untreated and CGRP-treated MDLCs with HSV-1 primary isolates, in the absence or presence of inhibitors of endolysosomal acidification, namely the lysosomotropic agent NH_4Cl and the inhibitor of ATPase H^+ pumps bafilomycin A1, and evaluated infection 24hr pi by flow cytometry. These experiments showed that in untreated MDLCs, the inhibitors had no effect on HSV-1 infection when included only during the 2hr viral pulse period (Figure 5E), but significantly inhibited HSV-1 infection when included during the 24hr CGRP treatment period (Figure 5F). In contrast, the inhibitors had no effect in CGRP-treated MDLCs, when added either during the pulse or CGRP treatment periods (Figure 5E, F).

Together, these results show that HSV-1 enters human LCs in 3-OS-dependent and pH-dependent manners. GCRP inhibits HSV-1 infection in LCs by potentially decreasing 3-OS HS surface expression and by abrogating the pH dependency required for infection.

CGRP inhibits langerin-dependent and pH-independent HSV-2 infection of human LCs

In addition to nectin-1, nectin-2 and HVEM that mediate HSV-2 entry, HSV-2 also binds and uses langerin as an entry receptor in LCs [21]. We therefore performed additional receptor blocking

239 experiments as above, using nAbs to HSV-2 entry receptors and langerin. These experiments showed
240 that pre-incubation with both nectin-1 and langerin nAbs significantly inhibited by approximately
241 15% and 50%, respectively, HSV-2 infection of untreated MDLCs, while the other nAbs had no
242 significant effect (Figure 6A). Of note, heparinase pre-treatment inhibited HSV-2 infection of
243 untreated MDLCs by approximately 20% (Figure 6A), which could be expected as HSV-2 uses HS,
244 but not 3-OS HS, as an early attachment receptor [35]. Importantly, in CGRP-treated MDLCs, pre-
245 incubation with the langerin nAb also reduced HSV-2 infection by approximately 50% (Figure 6B).
246 Similarly, pre-incubation with the langerin nAb significantly inhibited HSV-2 infection of both
247 untreated and CGRP-treated inner foreskin langerin^{high} LCs (Figure 6C). These results show that
248 HSV-2 uses langerin to enter untreated and CGRP-treated MDLCs and inner foreskin langerin^{high}
249 LCs.
250 We next investigated whether CGRP affects clathrin/caveolin-mediated endocytosis that is involved
251 in langerin internalization and recycling following ligand binding [36, 37], and determined the pH-
252 dependency of HSV-2 entry. Accordingly, untreated and CGRP-treated MDLCs were pulsed with
253 HSV-2 primary isolates for 2hr, in the absence or presence of dynasore (a dynamin inhibitor that
254 blocks clathrin-mediated endocytosis), methyl beta cyclodextrin (MβCD, a cholesterol depleting
255 agent that blocks caveolin-mediated endocytosis) or NH_4Cl and bafilomycin A1 as above. These
256 experiments showed that dynasore or MβCD reduced HSV-2 infection, in both untreated and CGRP-
257 treated MDLCs (Figure 6D and Supplementary Figure 8). In contrast, NH_4Cl and bafilomycin A1 had
258 no effect on HSV-2 infection in either untreated or CGRP-treated MDLCs (Figure 6E, F). These
259 results indicate that HSV-2 enters MDLCs via langerin-dependent pH-independent endocytosis.
260 As we previously reported, CGRP increases langerin expression in MDLCs [29]. To confirm these
261 observations and understand why langerin up-regulation appears to decrease rather than increase
262 HSV-2 entry in LCs, we investigated whether CGRP affects langerin trimeric structure [38]. Hence, we
263 cross-linked surface langerin in MDLCs using non-saturating concentration of a chemical cross-

linker, and evaluated langerin oligomeric status by Western blot. These experiments showed that langerin was dissociated into its monomeric form in untreated MDLCs in the absence of cross-linking (Figure 6G, lane 1). As expected, following cross-linking, langerin was present both as monomers and trimers, i.e. a band of approximately 120kDa that equals three langerin monomers (Figure 6G, lane 2). In line with our previous findings, CGRP significantly increased langerin expression in MDLCs (Figure 6G, lane 3). Surprisingly, in addition to langerin monomers and trimers, a langerin higher molecular weight band corresponding to double trimers of approximately 240kDa was detected in CGRP-treated and cross-linked MDLCs (Figure 6G, lane 4). These double trimers were significantly increased, while monomers were decreased and trimers remained unchanged, when comparing CGRP-treated to untreated MDLCs following cross-linking (Figure 6G, pie plots), suggesting *de-novo* formation of double trimers from monomers. Like CGRP, its metabolically stable analogue SAX also increased the expression of langerin double trimers in MDLCs (Supplementary Figure 9).

Together, these results show that HSV-2 enters MDLCs via langerin-mediated endocytosis and pH-independent mechanisms. CGRP might inhibit HSV-2 infection in MDLCs by inducing formation of atypical langerin trimers, which could prevent HSV-2 binding and subsequent entry.

Discussion

In the present study, we identified a novel mechanism limiting mucosal HSV infection, involving neuroimmune interactions between CGRP and human LCs, as schematically summarized in Figure 7. To the best of our knowledge, this is the first report of a protective anti-viral role of CGRP during human HSV infection.

We show that human MDLCs are HSV-1/2-permissive and that CGRP significantly inhibits their productive infection with both HSV-1 and HSV-2. Such inhibition is of approximately 50% at 24hr pi, and reaches around 70-75% at 48hr pi for both viruses, indicating that the effect of CGRP is long lasting. Similarly, inhibition of MDLCs-mediated HSV-1 and HSV-2 infection at 24hr pi by SAX, a metabolically stable peptide analogue of CGRP that has a longer half-life [39, 40], is more potent compared to CGRP. Hence, while SAX has lower potency than CGRP in inducing beneficial cardiovascular effects [40, 41], and inhibiting LCs-mediated HIV-1 transfer to $CD4^+$ T-cells as we recently reported [31], SAX might be preferable for potential clinical applications in the context of mucosal HSV infection.

In our experiments with human inner foreskin mucosal tissues, we could confirm the presence of two recently described LC subsets [24, 25], namely $CD1a^{high}langerin^{high}$ and $CD1a^{low}langerin^{low}$ LCs. In comparison, all MDLCs are $CD1a^{high}$ and a proportion of MDLCs expresses varying levels of langerin. Yet, langerin expression in MDLCs is a dynamic continuum that can be further increased depending on the *in-vitro* culture conditions, for instance in the absence of serum or short exposure to certain cytokines [42, 43]. We therefore speculate that MDLCs might be more representative of $CD1a^{high}langerin^{high}$ tissue LCs, which also corresponds with our findings that CGRP inhibits infection of inner foreskin $langerin^{high}$ cells with HSV-1 and HSV-2.

Inner foreskin $langerin^{low}$ LCs might represent the proportion of Epi-cDC2s that expresses langerin and/or the LC2 subset, which are readily found in inner foreskin but at very low frequency in skin [24,

306 [25]. Our langerin-based gating strategy might explain why we observed similar HSV-1 infection
307 degrees of langerin^{high} and langerin^{low} LCs in the inner foreskin, compared to the enhanced HSV-1
308 infection of langerin-negative Epi-cDC2s vs. langerin^{high} LCs recently reported in skin [32].
309 Interestingly, we found that CGRP has no effect on HSV-1 and HSV-2 infection of inner foreskin
310 langerin^{low} cells. As Epi-cDC2s transcriptionally resemble DCs and not LCs [24, 32], the lack of
311 inhibitory effect of CGRP on langerin^{low} cells might correlate with our observations, showing that
312 CGRP has no effect on monocyte-derived DCs (MDDCs)-mediated HIV-1 trans-infection [29] and
313 HSV-1/2 infection (data not shown). Further studies are now required in order to determine HSV-2
314 permissiveness of skin LCs vs. Epi-cDC2s, and investigate whether langerin^{low} vs. langerin^{neg} Epi-
315 cDC2s in the inner foreskin represent distinct cell populations.
316 We further show that HSV-1 and HSV-2 rely on the usage of different entry receptors in MDLCs,
317 namely the HSV-1-specific entry receptor 3-OS HS mediates HSV-1 infection, while langerin is the
318 primary receptor mediating HSV-2 infection, highlighting its crucial role in conferring HSV-2
319 permissiveness of MDLCs. As we could not obtain complete blocking of HSV-1/2 infection in
320 MDLCs when combining several nAbs simultaneously (data not shown), other surface receptors
321 could mediate viral entry in MDLCs (e.g. the C-type lectin DC-SIGN [44], expressed by MDLCs but
322 not tissue LCs, and potentially others that remain to be identified).
323 Although the yield of inner foreskin LCs is insufficient for full receptor neutralization experiments,
324 we found higher HSV-2 infection and confirmed langerin usage by HSV-2 in langerin^{high} inner
325 foreskin LCs. We could also show usage by HSV-1 in langerin^{high} inner foreskin LCs of both 3-OS
326 HS and langerin, the latter recently described for skin LCs [32]. As langerin does not seem to contribute
327 to HSV-1 infection in MDLCs, we speculate that such discrepancies could be explained in part by the
328 fact that MDLCs are >95% positive for 3-OS HS and only partially express langerin, while tissue LCs
329 are 100% positive for langerin and only partially express 3-OS HS (e.g. 25% of inner foreskin

langerin^{high} cells as we show herein). Such different receptors abundance might affect langerin vs. 3-OS HS usage for HSV-1 entry.

Our results further indicate that the inhibitory effects of CGRP in MDLCs are exerted by distinct mechanisms, related to the specific HSV-1 and HSV-2 entry receptors we identified.

For HSV-1, we found that the virus uses 3-OS HS to enter MDLC, and in a pH-dependent manner alike described for skin LCs [32]. We hence speculate that HSV-1 entry takes place via binding to 3-OS HS at the plasma membrane, leading to 3-OS HS clustering within lipid rafts and its internalization [45], followed by low pH endocytic escape of HSV-1 into the cytosol. In turn, CGRP pre-treatment inhibits HSV-1 infection of MDLCs by potentially affecting two different steps in this entry process, namely CGRP significantly decreases 3-OS HS expression and also abrogates pH dependency. Although the exact mechanism through which CGRP down-regulates 3-OS HS remains to be elucidated, it is possible that CGRP acts by interfering with the generation of 3-OS HS. For instance, HS is transformed by 3-O sulfotransferase (3-OST) to yield 3-OS HS [46], and CGRP could modulate 3-OST activity or its substrates. Other studies should also determine how CGRP interferes with the endolysosomal machinery and abrogates the need for low pH during HSV-1 infection, which might also be related to our previous results showing that CGRP diverts HIV-1 degradation away from endolysosomes [19].

For HSV-2, we found that infection of MDLCs occurs via langerin-mediated endocytosis in a pH-independent manner. HSV-2 is therefore probably internalized following its binding to langerin, and could be delivered to endocytic compartments and/or Birbeck granules, i.e. langerin-formed intracellular structures that are unique to LCs and are part of the endosomal recycling machinery [36]. As our previous studies showed that CGRP has no effect on langerin internalization [19], CGRP-mediated inhibition of HSV-2 infection probably occurs in a pre-entry step. Indeed, compared with langerin homo-trimers that are essential for efficient ligand binding [20] (e.g. including large pathogens such as HSV), we speculate that CGRP-induced atypical langerin double trimers might be less

efficient, and even defective, in ligand binding. Structural studies could reveal whether isolated langerin double trimers have steric interference for HSV-2 binding, leading to decreased HSV-2 internalization and infection.

Based on our results, we propose an original preventive neuro-immune approach, namely using CGRP-based formulations for inhibition of HSV-1/2 infection. As epidemiological and molecular studies indicate a synergistic relationship between HSV-2 and HIV-1 during co-infection [47], future CGRP-based formulations might represent an interesting alternative, i.e. by inhibiting LCs-mediated infection with both HSV and HIV-1 simultaneously. Collectively, our previous studies and the results reported herein reinforce the role and potential utility of CGRP, in the neuro-immune control of mucosal viral infections.

Methods

Ethical statement

The study was performed under local ethical approval (Comités de Protection des Personnes CPP Paris-IdF XI, N.11016) and all patients signed informed consents.

Viruses

HSV-1 and HSV-2 primary isolates were derived from genital lesions of HSV^+ patients and were obtained from the Virology Service at the Cochin Hospital, Paris, France. All primary isolates were amplified once in Vero cells, titrated via standard plaque assay, aliquoted and stored at -80°C.

MDLCs and inner foreskin LCs

Peripheral blood mononuclear cells (PBMCs) from healthy HIV-1 seronegative individuals, $CD14^+$ monocytes and MDLCs were separated as we previously described [29].

Normal foreskin tissues were derived from healthy adults undergoing circumcision and were obtained from the Urology Service at the Cochin Hospital, Paris, France. Inner foreskin epidermal cell suspensions were prepared using enzymatic digestion with dispase / trypsin, as we described [15, 18]. For receptor blocking experiments, suspensions were enriched for immune cells using Ficoll gradient.

Flow cytometry

To characterize their phenotype or expression of HSV entry receptors, MDLCs or inner foreskin epidermal cells ($0.5\text{-}1x10^5$ / well, in duplicates in round bottom 96-wells plate) were stained for 20min on ice in a final volume of 50µl phosphate-buffered saline (PBS) with the Abs indicated in Supplementary Table 1. Matched isotype control Abs were included for HSV entry receptors

experiments and fluorescent profiles were acquired using a Guava easyCite and analyzed with the InCyte software (Merck-Millipore).

HSV infection and apoptosis/viability

MDLCs or inner foreskin epidermal cell suspensions ($0.5x10^5$ MDLCs and $2x10^5$ epidermal cells / 200µl / well, in duplicates in round bottom 96-wells plates) were re-suspended in complete RPMI medium. Cells were either left untreated or pre-treated for 24hr at 37°C with the indicated molar concentrations of CGRP (AnaSpec), or the metabolically stable CGRP analogue SAX we described and prepared [39, 40]. The cells were then re-suspended in RPMI medium without serum and pulsed for 2hr (MDLCs) or 24hr (inner foreskin epidermal cells) at 37°C with primary isolates of either HSV-1 or HSV-2 at the indicated MOIs. In some experiments with MDLCs, the following inhibitors (Sigma) were included: NH_4Cl (10mM), bafilomycin A1 (10nM), dynasore (100µM), methyl beta cyclodextrin (10mM). Of note, at the concentrations / time point tested, none of the agonists and inhibitors affected MDLCs viability, as evaluated below. The medium-containing virus was then removed, the cells were washed and further incubated at 37°C in complete RPMI medium. At 24 and 48hr pi, cells were washed with 0.1M glycine buffer pH=2.0 for 2min at room temperature in order to detach non-internalized HSV virions. Cells were then surface-stained for langerin expression as above, fixed with PBS / 4% paraformaldehyde (PFA, Electron Microscopy Sciences), washed, permeabilized with PBS / 0.1% saponin, and intracellularly stained for 20min at room temperature for HSV-1/2-gD expression (see Supplementary Table 1). Cells were then analyzed by flow cytometry as above. Apoptosis and viability of non-infected and HSV-infected MDLCs were evaluated by Annexin / PI staining using an Annexin V-FITC kit or Viobility Fixable Dye staining (Miltenyi Biotec), according to the manufacturer's instructions.

HSV receptors blocking assay

MDLCs or inner foreskin epidermal cell suspensions that were enriched for immune cells ($0.5x10^5$ cells / well, in duplicates in round bottom 96-wells plate) were pre-incubated for 1hr at 37°C in a final volume of 25µl PBS with the nAbs indicated in Supplementary table 1. Of note, we verified that the langerin nAb does not interfere with langerin detection using the DCGM4 clone (data not shown). Cells were also incubated with 10U/ml of heparinase II and/or II (from *Flavobacterium heparinum*; Sigma). Next, cells were then washed and infected with HSV-1 or HSV-2, as above.

Cross-linking and Western blot

MDLCs ($2.5x10^6$ cells / 5ml / T25 flasks) were either left untreated or treated for 24hr at 37°C with 1µM CGRP or SAX. Cells were then cross-linked as previously described [20], using the chemical cross linker disuccinimidyl glutamarate (DSG, ChemCruz) that was dissolved in Dimethyl sulfoxide (DMSO) and added to the suspensions at 1mM for 30min at room temperature. Samples (25µg protein / sample) were run over a 10% SDS-PAGE, transferred onto nitrocellulose membranes at 4°C, and membranes were blocked with blocking buffer (TBS / 0.5% Tween 20 / 0.5% dry milk) for 1hr at room temperature with constant agitation. Membranes were next incubated overnight at 4°C with 0.1µg/ml goat polyclonal anti-human langerin IgG Ab (R&D Systems), followed by 0.5µg/ml horse-radish-peroxidase-conjugated donkey anti-goat polyclonal Ab (Promega), diluted in blocking buffer. Revelation was performed with ECL-Prime chemiluminescence detection kit (Amersham). Images were acquired with the Fusion FX camera platform (Vilber Lournmat) and expression quantified with the ImageJ software.

Statistical analysis

Statistical significance was analyzed by two-tailed Student's t-test or ANOVA. The relationships between HSV infection and replication were analyzed with Pearson correlations.

Acknowledgments

This study was funded by a research grant (to Y.G.) and PhD fellowships (to E.C. and J.M.) from Agence Nationale de la Recherches sur le Sida et les Hépatites virales (ANRS) | Maladies Infectieuses Émergentes, and by a research grant (to M.B.) from Fondation pour la Recherche Medicale (FRM).

Author contributions

E.C., J.M. and Y.G. performed the experiments; F.R. provided primary HSV isolates; A.S. prepared and provided SAX; T.H.vK prepared and provided clone HS4C3 against 3-OS HS; N.B.D. and M.Z. provided foreskin tissues; Y.G. and M.B. designed the experiments; Y.G. conceived the study and wrote the paper.

Conflict of interest

The authors declare no conflict of interest.

References

1. James C, Harfouche M, Welton NJ, Turner KM, Abu-Raddad LJ, Gottlieb SL *et al.* Herpes simplex virus: global infection prevalence and incidence estimates, 2016. *Bull World Health Organ* 2020; **98**(5)**:** 315-329.

2. Johnston C, Gottlieb SL, Wald A. Status of vaccine research and development of vaccines for herpes simplex virus. *Vaccine* 2016; **34**(26)**:** 2948-2952.

3. Desai DV, Kulkarni SS. Herpes Simplex Virus: The Interplay Between HSV, Host, and HIV-1. *Viral Immunol* 2015; **28**(10)**:** 546-555.

4. Lafferty WE, Downey L, Celum C, Wald A. Herpes simplex virus type 1 as a cause of genital herpes: impact on surveillance and prevention. *J Infect Dis* 2000; **181**(4)**:** 1454-1457.

5. Masese L, Baeten JM, Richardson BA, Bukusi E, John-Stewart G, Graham SM *et al.* Changes in the contribution of genital tract infections to HIV acquisition among Kenyan high-risk women from 1993 to 2012. *AIDS* 2015; **29**(9)**:** 1077-1085.

6. Roizman B, Knipe DM, J. WR. Herpes Simplex Virus. In: Knipe DM, Howley PM (eds). *Fields Virology*. Wolters Kluwer Health/ Lippincott William & Wilkins: Philadelphia, 2013.

7. Russell FA, King R, Smillie SJ, Kodji X, Brain SD. Calcitonin gene-related peptide: physiology and pathophysiology. *Physiol Rev* 2014; **94**(4)**:** 1099-1142.

8. Flowerdew SE, Wick D, Himmelein S, Horn AK, Sinicina I, Strupp M *et al.* Characterization of neuronal populations in the human trigeminal ganglion and their association with latent herpes simplex virus-1 infection. *PLoS One* 2013; **8**(12)**:** e83603.

9. Cabrera JR, Charron AJ, Leib DA. Neuronal Subtype Determines Herpes Simplex Virus 1 Latency-Associated-Transcript Promoter Activity during Latency. *J Virol* 2018; **92**(13).

10. Hamza MA, Higgins DM, Ruyechan WT. Two alphaherpesvirus latency-associated gene products influence calcitonin gene-related peptide levels in rat trigeminal neurons. *Neurobiol Dis* 2007; **25**(3)**:** 553-560.

11. Margolis TP, Imai Y, Yang L, Vallas V, Krause PR. Herpes simplex virus type 2 (HSV-2) establishes latent infection in a different population of ganglionic neurons than HSV-1: role of latency-associated transcripts. *J Virol* 2007; **81**(4)**:** 1872-1878.

12. Truong NR, Smith JB, Sandgren KJ, Cunningham AL. Mechanisms of Immune Control of Mucosal HSV Infection: A Guide to Rational Vaccine Design. *Front Immunol* 2019; **10:** 373.

13. de Jong MA, de Witte L, Oudhoff MJ, Gringhuis SI, Gallay P, Geijtenbeek TB. TNF-alpha and TLR agonists increase susceptibility to HIV-1 transmission by human Langerhans cells ex vivo. *J Clin Invest* 2008; **118**(10)**:** 3440-3452.

14. de Witte L, Nabatov A, Pion M, Fluitsma D, de Jong MA, de Gruijl T *et al.* Langerin is a natural barrier to HIV-1 transmission by Langerhans cells. *Nat Med* 2007; **13**(3)**:** 367-371.

15. Ganor Y, Zhou Z, Tudor D, Schmitt A, Vacher-Lavenu MC, Gibault L *et al.* Within 1 h, HIV-1 uses viral synapses to enter efficiently the inner, but not outer, foreskin mucosa and engages Langerhans-T cell conjugates. *Mucosal Immunol* 2010; **3**(5)**:** 506-522.

16. Hladik F, Sakchalathorn P, Ballweber L, Lentz G, Fialkow M, Eschenbach D *et al.* Initial events in establishing vaginal entry and infection by human immunodeficiency virus type-1. *Immunity* 2007; **26**(2)**:** 257-270.

17. Kawamura T, Cohen SS, Borris DL, Aquilino EA, Glushakova S, Margolis LB *et al.* Candidate microbicides block HIV-1 infection of human immature Langerhans cells within epithelial tissue explants. *The Journal of experimental medicine* 2000; **192**(10)**:** 1491-1500.

18. Zhou Z, Barry de Longchamps N, Schmitt A, Zerbib M, Vacher-Lavenu MC, Bomsel M *et al.* HIV-1 Efficient Entry in Inner Foreskin Is Mediated by Elevated CCL5/RANTES that Recruits T Cells and Fuels Conjugate Formation with Langerhans Cells. *PLoS Pathog* 2011; **7**(6)**:** e1002100.

19. Bomsel M, Ganor Y. Calcitonin Gene-Related Peptide Induces HIV-1 Proteasomal Degradation in Mucosal Langerhans Cells. *J Virol* 2017; **91**(23)**:** e01205-01217.

20. Nasr N, Lai J, Botting RA, Mercier SK, Harman AN, Kim M *et al.* Inhibition of two temporal phases of HIV-1 transfer from primary Langerhans cells to T cells: the role of langerin. *J Immunol* 2014; **193**(5)**:** 2554-2564.

21. de Jong MA, de Witte L, Taylor ME, Geijtenbeek TB. Herpes simplex virus type 2 enhances HIV-1 susceptibility by affecting Langerhans cell function. *J Immunol* 2010; **185**(3)**:** 1633-1641.

22. Marsden V, Donaghy H, Bertram KM, Harman AN, Nasr N, Keoshkerian E *et al.* Herpes simplex virus type 2-infected dendritic cells produce TNF-alpha, which enhances CCR5 expression and stimulates HIV production from adjacent infected cells. *J Immunol* 2015; **194**(9)**:** 4438-4445.

23. Ogawa Y, Kawamura T, Matsuzawa T, Aoki R, Gee P, Yamashita A *et al.* Antimicrobial peptide LL-37 produced by HSV-2-infected keratinocytes enhances HIV infection of Langerhans cells. *Cell Host Microbe* 2013; **13**(1)**:** 77-86.

24. Bertram KM, Botting RA, Baharlou H, Rhodes JW, Rana H, Graham JD *et al.* Identification of HIV transmitting CD11c(+) human epidermal dendritic cells. *Nat Commun* 2019; **10**(1)**:** 2759.

25. Liu X, Zhu R, Luo Y, Wang S, Zhao Y, Qiu Z *et al.* Distinct human Langerhans cell subsets orchestrate reciprocal functions and require different developmental regulation. *Immunity* 2021; **54**(10)**:** 2305-2320 e2311.

26. Baral P, Udit S, Chiu IM. Pain and immunity: implications for host defence. *Nat Rev Immunol* 2019; **19**(7)**:** 433-447.

27. Granstein RD, Wagner JA, Stohl LL, Ding W. Calcitonin gene-related peptide: key regulator of cutaneous immunity. *Acta physiologica* 2015; **213**(3)**:** 586-594.

28. Ganor Y, Drillet-Dangeard AS, Bomsel M. Calcitonin gene-related peptide inhibits human immunodeficiency type 1 transmission by Langerhans cells via an autocrine/paracrine feedback mechanism. *Acta physiologica* 2015; **213**(2)**:** 432-441.

29. Ganor Y, Drillet-Dangeard AS, Lopalco L, Tudor D, Tambussi G, Delongchamps NB *et al.* Calcitonin gene-related peptide inhibits Langerhans cell-mediated HIV-1 transmission. *The Journal of experimental medicine* 2013; **210**(11)**:** 2161-2170.

30. Agelidis AM, Shukla D. Cell entry mechanisms of HSV: what we have learned in recent years. *Future Virol* 2015; **10**(10)**:** 1145-1154.

31. Mariotton J, Sams A, Cohen E, Sennepin A, Siracusano G, Sanvito F *et al.* Native CGRP Neuropeptide and Its Stable Analogue SAX, But Not CGRP Peptide Fragments, Inhibit Mucosal HIV-1 Transmission. *Front Immunol* 2021; **12:** 785072.

32. Bertram KM, Truong NR, Smith JB, Kim M, Sandgren KJ, Feng KL *et al.* Herpes Simplex Virus type 1 infects Langerhans cells and the novel epidermal dendritic cell, Epi-cDC2s, via different entry pathways. *PLoS Pathog* 2021; **17**(4)**:** e1009536.

33. Ten Dam GB, Kurup S, van de Westerlo EM, Versteeg EM, Lindahl U, Spillmann D *et al.* 3-O-sulfated oligosaccharide structures are recognized by anti-heparan sulfate antibody HS4C3. *J Biol Chem* 2006; **281**(8)**:** 4654-4662.

34. Madavaraju K, Koganti R, Volety I, Yadavalli T, Shukla D. Herpes Simplex Virus Cell Entry Mechanisms: An Update. *Front Cell Infect Microbiol* 2020; **10:** 617578.

35. Shukla D, Spear PG. Herpesviruses and heparan sulfate: an intimate relationship in aid of viral entry. *J Clin Invest* 2001; **108**(4)**:** 503-510.

36. Mc Dermott R, Ziylan U, Spehner D, Bausinger H, Lipsker D, Mommaas M *et al.* Birbeck granules are subdomains of endosomal recycling compartment in human epidermal Langerhans cells, which form where Langerin accumulates. *Mol Biol Cell* 2002; **13**(1)**:** 317-335.

37. van den Berg LM, Ribeiro CM, Zijlstra-Willems EM, de Witte L, Fluitsma D, Tigchelaar W *et al.* Caveolin-1 mediated uptake via langerin restricts HIV-1 infection in human Langerhans cells. *Retrovirology* 2014; **11:** 123.

38. Stambach NS, Taylor ME. Characterization of carbohydrate recognition by langerin, a C-type lectin of Langerhans cells. *Glycobiology* 2003; **13**(5)**:** 401-410.

39. Nilsson C, Hansen TK, Rosenquist C, Hartmann B, Kodra JT, Lau JF *et al.* Long acting analogue of the calcitonin gene-related peptide induces positive metabolic effects and secretion of the glucagon-like peptide-1. *Eur J Pharmacol* 2016; **773:** 24-31.

40. Sheykhzade M, Abdolalizadeh B, Koole C, Pickering DS, Dreisig K, Johansson SE *et al.* Vascular and molecular pharmacology of the metabolically stable CGRP analogue, SAX. *Eur J Pharmacol* 2018; **829:** 85-92.

41. Aubdool AA, Thakore P, Argunhan F, Smillie SJ, Schnelle M, Srivastava S *et al.* A Novel alpha-Calcitonin Gene-Related Peptide Analogue Protects Against End-Organ Damage in Experimental Hypertension, Cardiac Hypertrophy, and Heart Failure. *Circulation* 2017; **136**(4)**:** 367-383.

42. Otsuka Y, Watanabe E, Shinya E, Okura S, Saeki H, Geijtenbeek TBH *et al.* Differentiation of Langerhans Cells from Monocytes and Their Specific Function in Inducing IL-22-Specific Th Cells. *J Immunol* 2018; **201**(10)**:** 3006-3016.

43. Picarda G, Cheneau C, Humbert JM, Beriou G, Pilet P, Martin J *et al.* Functional Langerinhigh-Expressing Langerhans-like Cells Can Arise from CD14highCD16- Human Blood Monocytes in Serum-Free Condition. *J Immunol* 2016; **196**(9)**:** 3716-3728.

44. de Jong M, de Witte L, Bolmstedt A, van Kooyk Y, Geijtenbeek TBH. Dendritic cells mediate herpes simplex virus infection and transmission through the C-type lectin DC-SIGN. *J Gen Virol* 2008; **89**(Pt 10)**:** 2398-2409.

45. Christianson HC, Belting M. Heparan sulfate proteoglycan as a cell-surface endocytosis receptor. *Matrix Biol* 2014; **35:** 51-55.

46. Shworak NW, Liu J, Petros LM, Zhang L, Kobayashi M, Copeland NG *et al.* Multiple isoforms of heparan sulfate D-glucosaminyl 3-O-sulfotransferase. Isolation, characterization, and expression of human cdnas and identification of distinct genomic loci. *J Biol Chem* 1999; **274**(8)**:** 5170-5184.

47. Looker KJ, Elmes JAR, Gottlieb SL, Schiffer JT, Vickerman P, Turner KME *et al.* Effect of HSV-2 infection on subsequent HIV acquisition: an updated systematic review and meta-analysis. *Lancet Infect Dis* 2017; **17**(12)**:** 1303-1316.

646 **Figure legends**

647

648 **Figure 1. Human LCs express HSV-1 and HSV-2 entry receptors.** Monocytes **(A)**, MDLCs **(B)**,
649 or inner foreskin epidermal cell suspensions **(C)**, were labeled for cell-surface expression of HSV-1/2
650 entry receptors and langerin. Matched isotype control Abs (broken lines) served as negative controls,
651 and cells were examined by flow cytometry. Shown are representative flow cytometry overlays, with
652 numbers representing mean±SEM (n=4-9, see Supplementary Figure 2) percentages of positive cells
653 out of total cells (A) or gated on langerin$^+$ cells (B, C).

654

655 **Figure 2. Human MDLCs are productively infected with HSV-1 and HSV-2. (A-D)** MDLCs were
656 pulsed for 2hr with different primary isolates of HSV-1 or HSV-2, and infection was examined 24-
657 48hr pi by flow cytometry. In (A, B), shown are representative flow cytometry dot-plots of MDLCs
658 infected with HSV-1 or HSV-2 vs. no HSV control, and examined immediately following the 2hr
659 viral pulse (A) or 24hr pi (B). Numbers represent percentages of langerin$^+$HSV-1/2-gD$^-$ (upper left
660 regions) and langerin$^+$HSV-1/2-gD$^+$ (upper right regions) cells. In (C, D), shown are mean±SEM
661 percentages of infection, calculated as ([langerin$^+$HSV-1/2-gD$^+$ MDLCs] / [total langerin$^+$ MDLCs] x
662 100), for each isolate tested at the indicated MOIs and examined at 24hr pi (C), and for MDLCs
663 pulsed with HSV-1 (isolate 3 at MOI=1.0) or HSV-2 (isolates 6/7 at MOI=0.5) and examined 24-48hr
664 pi (D). Dots (for HSV-1) or triangles (for HSV-2) represent independent experiments, using MDLCs
665 from different individuals. **(E)** MDLCs were pulsed for 2hr with HSV-1 (isolate 2 at MOI=0.2 and
666 isolate 3 at MOI=1.0) or HSV-2 (isolates 6/7 at MOI=0.5). At 24hr pi, infection was examined by
667 flow cytometry and replication was determined by plaque assay of the culture supernatants. Lines
668 denote linear correlations between HSV-1/2 infection percentages and plaque forming units (pfu) / ml
669 released into the culture supernatants, with r and p values derived from Pearson correlations. **(F)**
670 MDLCs were pulsed for 2hr with HSV-1 (isolate 3 at MOI=1.0) or HSV-2 (isolates 6/7 at MOI=0.5)

and apoptosis was examined 24-72hr pi by flow cytometry. Shown are mean±SEM (derived from n=7 independent experiments using MDLCs from different donors) percentages of apoptosis, calculated as ([langerin$^+$Annexin$^+$PI$^-$ MDLCs] / [total langerin$^+$ MDLCs] x 100). In all graphs, **p<0.0050; two-tailed Student's t-test.

Figure 3. Human inner foreskin langerin-expressing cells are productively infected with HSV-1 and HSV-2. Inner foreskin epidermal cell suspensions were pulsed for 24hr with primary isolates of HSV-1 (isolate 3) or HSV-2 (isolate 8) at MOI=10.0, stained at 48hr pi for surface langerin and intracellular HSV-1/2-gD, and examined by flow cytometry. **(A)** Representative flow cytometry dot-plots of suspensions infected with HSV-1 or HSV-2 vs. no HSV control, with numbers representing percentages of langerin^{high}HSV-1/2$^-$ (upper left regions), langerin^{high}HSV-1/2$^+$ (upper right regions), langerin^{low}HSV-1/2$^-$ (middle left regions) and langerin^{low}HSV-1/2$^+$ (middle right regions) cells. **(B)** Matched infection percentages of inner foreskin langerin^{high} (dark grey) vs. langerin^{low} (light grey) cells, infected with either HSV-1 (dots) or HSV-2 (triangles). For HSV-2, **p=0.0023; paired two-tailed Student's t-test.

Figure 4. CGRP inhibits human LCs infection with HSV-1 and HSV-2. (A-D) MDLCs were left untreated or pre-treated for 24hr with CGRP and SAX at the indicated molar concentrations (A, B), or with 100nM CGRP (C, D). Cells were then pulsed for 2hr with primary isolates of HSV-1 (isolate 2 at MOI=0.2 and isolate 3 at MOI=1.0) or HSV-2 (isolates 6/7 at MOI=0.5), and further incubated for 24hr (A, B) or 24-48hr (C, D). HSV-1/2 infection was examined by flow cytometry and replication was determined by plaque assay of the culture supernatants. Results represent mean±SEM (n=3-4) percentages of infection (A-C) or replication (D), normalized against untreated cells serving as the 100% set point. **(E, F)** Inner foreskin epidermal cell suspensions were left untreated or pre-treated for 24hr with 1μM CGRP, pulsed for 24hr with HSV-1 (isolate 3) or HSV-2 (isolate 8) at

MOI=10.0, and infection was examined 48h pi by flow cytometry. Results represent mean±SEM (derived from n=6 independent experiments using tissues from different donors) normalized percentages of infection of langerin^{high} (E) and langerin^{low} (F) cells. In all graphs, *p<0.0500, **p<0.0050 and ***p<0.0005 vs. untreated; two-tailed Student's t-test.

Figure 5. CGRP decreases 3-OS HS expression and abrogates pH dependency during HSV-1 infection of human LCs. (A, B) Untreated or CGRP-treated MDLCs were pre-incubated for 1hr at 37°C with nAbs to nectin-1, HVEM, PILR-α or langerin vs. matched isotype non-neutralizing control Abs, or pre-incubated with heparinase II/III vs. medium. Cells were then pulsed for 2hr with HSV-1 (isolate 3 at MOI=1.0) and infection was examined 24hr pi by flow cytometry. Results represent mean±SEM percentages of HSV-1 infection inhibition (A, n=7) or normalized (B, n=5). **(C)** Representative flow cytometry overlay, showing surface expression of 3-OS HS in untreated (empty histogram) and CGRP-treated (filled grey histogram) MDLCs vs. isotype control (broken line). Numbers represent mean±SEM (n=3) MFIs of 3-OS HS expression, gated on langerin^{+} MDLCs. **(D)** Untreated or CGRP-treated inner foreskin epidermal cell suspensions were pre-incubated for 1hr at 37°C with heparinase II+III or langerin nAb. Cells were then pulsed for 24hr with HSV-1 (isolate 3 at MOI=10.0), and infection was examined 48h pi by flow cytometry. Results represent mean±SEM (using n=3 tissues from different individuals) normalized percentages of HSV-1 infection. **(E, F)** Untreated or CGRP-treated MDLCs were pulsed with HSV-1 (isolates 1 at MOI=0.1 and isolate 2 at MOI=0.2), alone or in the presence of NH_4Cl or bafilomycin A1 during the 2hr pulse period (E) or 24hr CGRP treatment period (F), and infection was measured 24hr pi by flow cytometry. Results represent mean±SEM (n=3-5) normalized percentages of HSV-1 infection. In all graphs, *p<0.0500, **p<0.0050 and ***p<0.0005; two-tailed Student's t-test.

720 **Figure 6. CGRP inhibits langerin-mediated HSV-2 infection of human LCs and induces**
721 **atypical langerin double trimers. (A, B)** Untreated or CGRP-treated MDLCs were pre-incubated
722 for 1hr at 37°C with nAbs to nectin-1, nectin-2, HVEM or langerin vs. matched isotype non-
723 neutralizing control Abs, or pre-incubated with heparinase II/III vs. medium. Cells were then pulsed
724 for 2hr with HSV-2 (isolates 6 at MOI=0.5 and isolate 8 at MOI=2.5) and infection was examined
725 24hr pi by flow cytometry. Results represent mean±SEM percentages of HSV-2 infection inhibition
726 (A, n=8) or normalized (B, n=6). **(C)** Untreated or CGRP-treated inner foreskin epidermal cell
727 suspensions were pre-incubated for 1hr at 37°C with langerin nAb, pulsed for 24hr with HSV-2
728 (isolate 7 at MOI=10.0), and infection was examined 48h pi by flow cytometry. Results represent
729 mean±SEM (using n=3 tissues from different individuals) normalized percentages of HSV-2
730 infection. **(D-F)** Untreated or CGRP-treated MDLCs were pulsed with HSV-2 (isolate 4 at MOI=0.1
731 and isolate 7 at MOI=0.5), alone or in the presence of dynasore, NH_4Cl or bafilomycin A1 as
732 indicated, and infection was measured 24hr pi by flow cytometry. Results represent mean±SEM
733 (n=5) normalized percentages of HSV-2 infection. In all graphs, *p<0.0500, **p<0.0050 and
734 ***p<0.0005; two-tailed Student's t-test. **(G)** Representative Western blot showing langerin
735 expression in untreated (lane 1), untreated / DSG cross-linked (lane 2), CGRP-treated (lane 3), and
736 CGRP-treated / DSG cross-linked (lane 4) MDLCs. Langerin appears as ~47kDa monomers,
737 ~120kDa trimers and ~240 double trimers. Pie charts (representative of n=4 experiments) show
738 quantitative analysis of the proportions of each langerin form (p=0.0038, ANOVA, untreated vs.
739 CGRP-treated).
740
741 **Figure 7. Summary of HSV-1 and HSV-2 infection mechanisms in human LCs, and their**
742 **inhibition by CGRP.** (1) Human inner foreskin LCs and MDLCs express HSV-1/2 entry receptors
743 and langerin; (2) HSV-1 uses 3-OS HS to enter MDLCs via a pH-dependent endocytic mechanism, as
744 well as langerin in inner foreskin langerin^{high} LCs (broken line); (3) CGRP might inhibit HSV-1

infection by down-regulating 3-OS HS surface expression and abrogating pH dependency; (4) HSV-2 uses langerin to enter LCs, leading to clathrin/caveolin-mediated internalization and fusion in a pH-independent manner; (5) CGRP might inhibit HSV-2 infection by inducing formation of atypical high molecular weigh langerin double trimers.

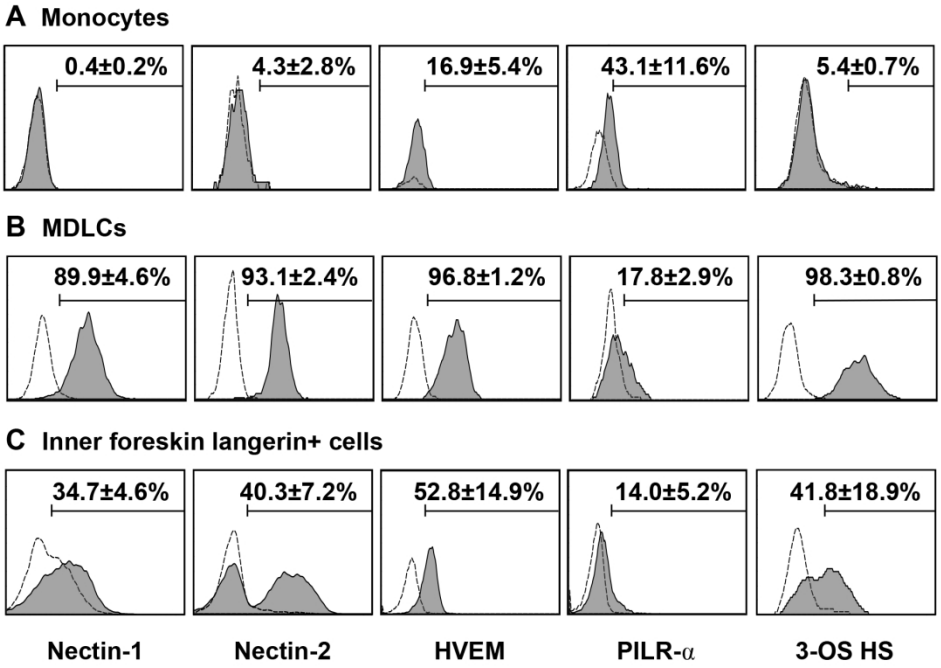
A Monocytes
0.4±0.2%
4.3±2.8%
16.9±5.4%
43.1±11.6%
5.4±0.7%
B MDLCs
89.9±4.6%
93.1±2.4%
96.8±1.2%
17.8±2.9%
98.3±0.8%
C Inner foreskin langerin+ cells
34.7±4.6%
40.3±7.2%
52.8±14.9%
14.0±5.2%
41.8±18.9%
Nectin-1
Nectin-2
HVEM
PILR-α
3-OS HS

Figure1

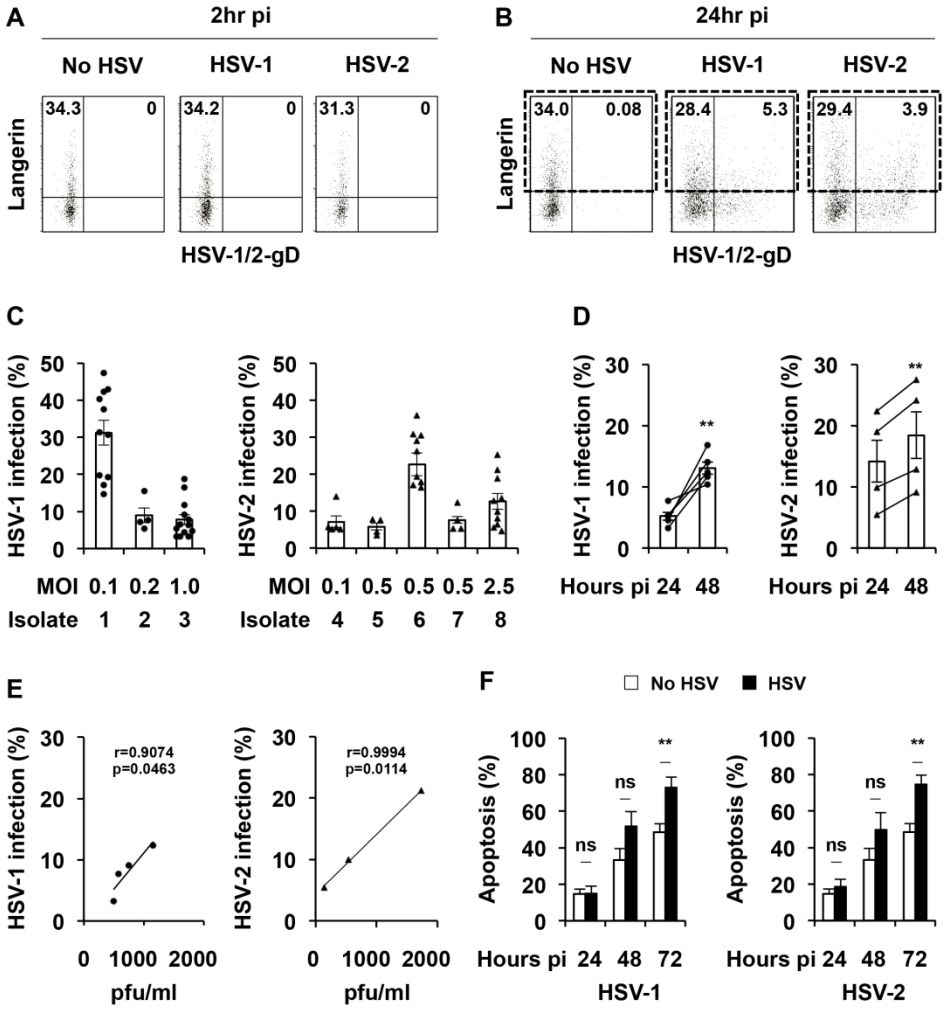
A
2hr pi
No HSV
HSV-1
HSV-2
Langerin
34.3
0
34.2
0
31.3
0
HSV-1/2-gD
B
24hr pi
No HSV
HSV-1
HSV-2
Langerin
34.0
0.08
28.4
5.3
29.4
3.9
HSV-1/2-gD
C
HSV-1 infection (%)
HSV-2 infection (%)
MOI 0.1 0.2 1.0
Isolate 1 2 3
MOI 0.1 0.5 0.5 0.5 2.5
Isolate 4 5 6 7 8
D
HSV-1 infection (%)
HSV-2 infection (%)
Hours pi 24 48
Hours pi 24 48
**
E
HSV-1 infection (%)
HSV-2 infection (%)
r=0.9074
p=0.0463
r=0.9994
p=0.0114
pfu/ml
pfu/ml
F
No HSV
HSV
Apoptosis (%)
Apoptosis (%)
ns
**
Hours pi 24 48 72
Hours pi 24 48 72
HSV-1
HSV-2

Figure2

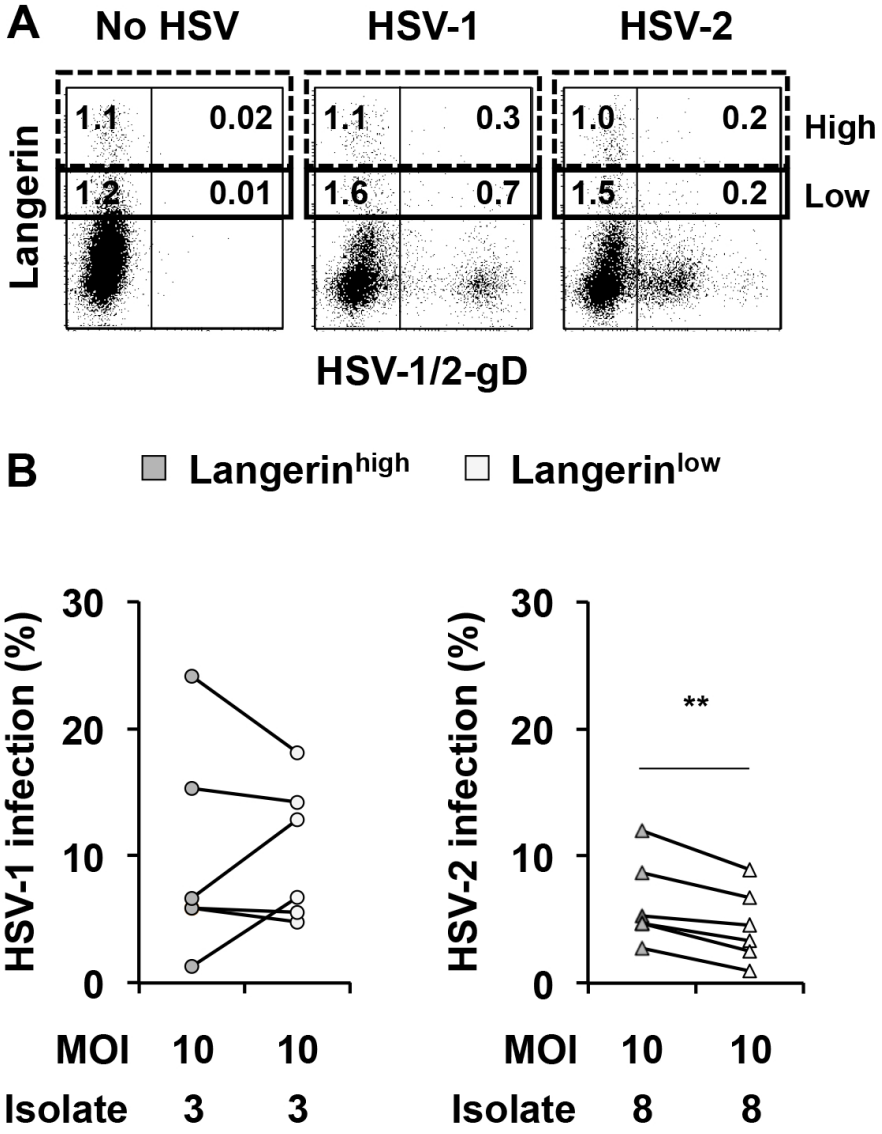
A
No HSV
HSV-1
HSV-2
Langerin
1.1
0.02
1.2
0.01
1.1
0.3
1.6
0.7
1.0
0.2
1.5
0.2
High
Low
HSV-1/2-gD
B
Langerin^high
Langerin^low
HSV-1 infection (%)
HSV-2 infection (%)
30
20
10
0
**
MOI 10 10
Isolate 3 3
MOI 10 10
Isolate 8 8

Figure3

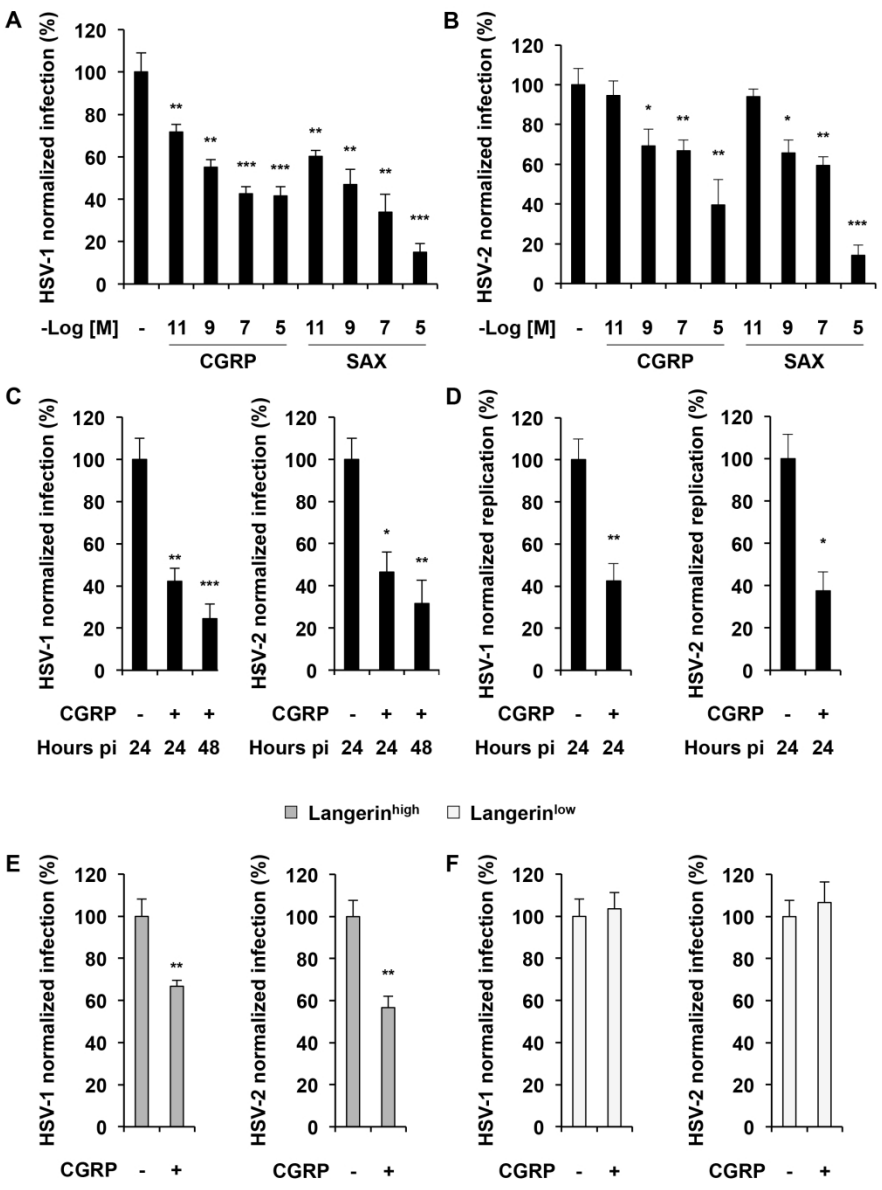
A
HSV-1 normalized infection (%)
-Log [M] - 11 9 7 5 11 9 7 5
CGRP
SAX
B
HSV-2 normalized infection (%)
-Log [M] - 11 9 7 5 11 9 7 5
CGRP
SAX
C
HSV-1 normalized infection (%)
CGRP - + +
Hours pi 24 24 48
HSV-2 normalized infection (%)
CGRP - + +
Hours pi 24 24 48
D
HSV-1 normalized replication (%)
CGRP - +
Hours pi 24 24
HSV-2 normalized replication (%)
CGRP - +
Hours pi 24 24
Langerin^high
Langerin^low
E
HSV-1 normalized infection (%)
CGRP - +
HSV-2 normalized infection (%)
CGRP - +
F
HSV-1 normalized infection (%)
CGRP - +
HSV-2 normalized infection (%)
CGRP - +

Figure4

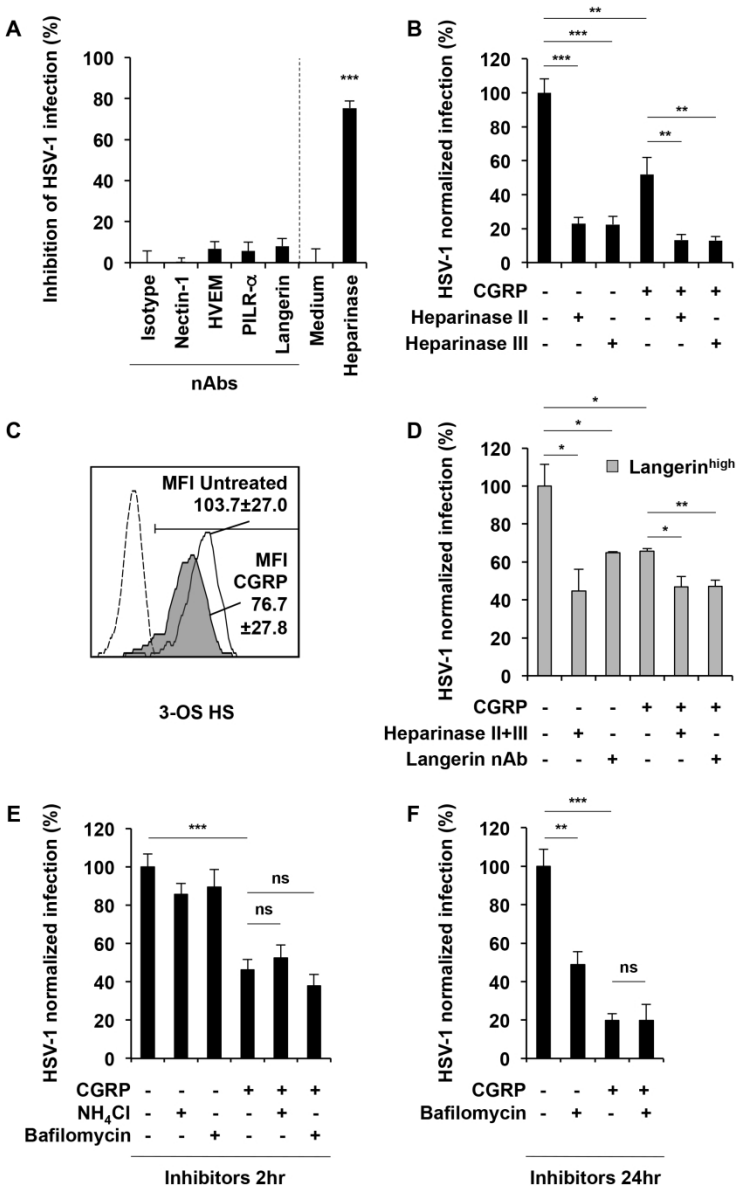

Figure5 revised

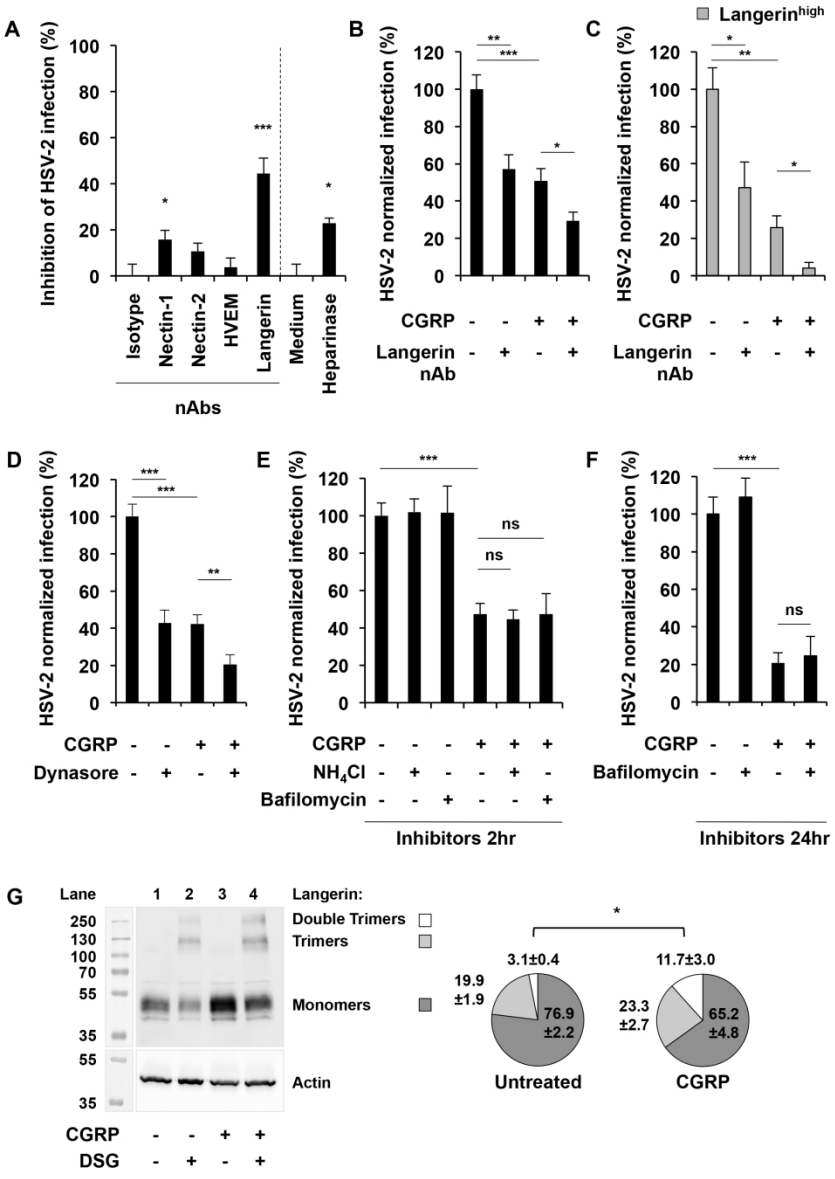
A
Inhibition of HSV-2 infection (%)
Isotype
Nectin-1
Nectin-2
HVEM
Langerin
Medium
Heparinase
nAbs
B
HSV-2 normalized infection (%)
CGRP
Langerin nAb
C
Langerin^high
HSV-2 normalized infection (%)
CGRP
Langerin nAb
D
HSV-2 normalized infection (%)
CGRP
Dynasore
E
HSV-2 normalized infection (%)
ns
CGRP
NH4Cl
Bafilomycin
Inhibitors 2hr
F
HSV-2 normalized infection (%)
ns
CGRP
Bafilomycin
Inhibitors 24hr
G
Lane
1 2 3 4
250
130
100
70
55
35
55
35
Langerin:
Double Trimers
Trimers
Monomers
Actin
CGRP
DSG
3.1±0.4
19.9 ±1.9
76.9 ±2.2
Untreated
11.7±3.0
23.3 ±2.7
65.2 ±4.8
CGRP

Figure6

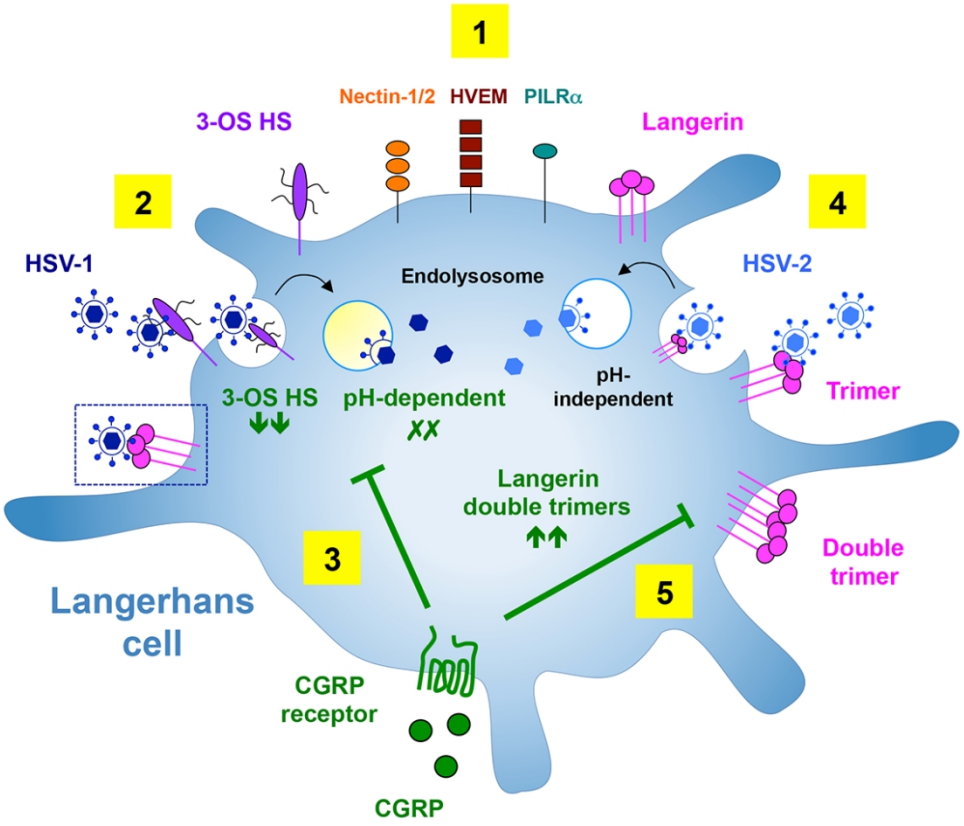

Figure7 revised

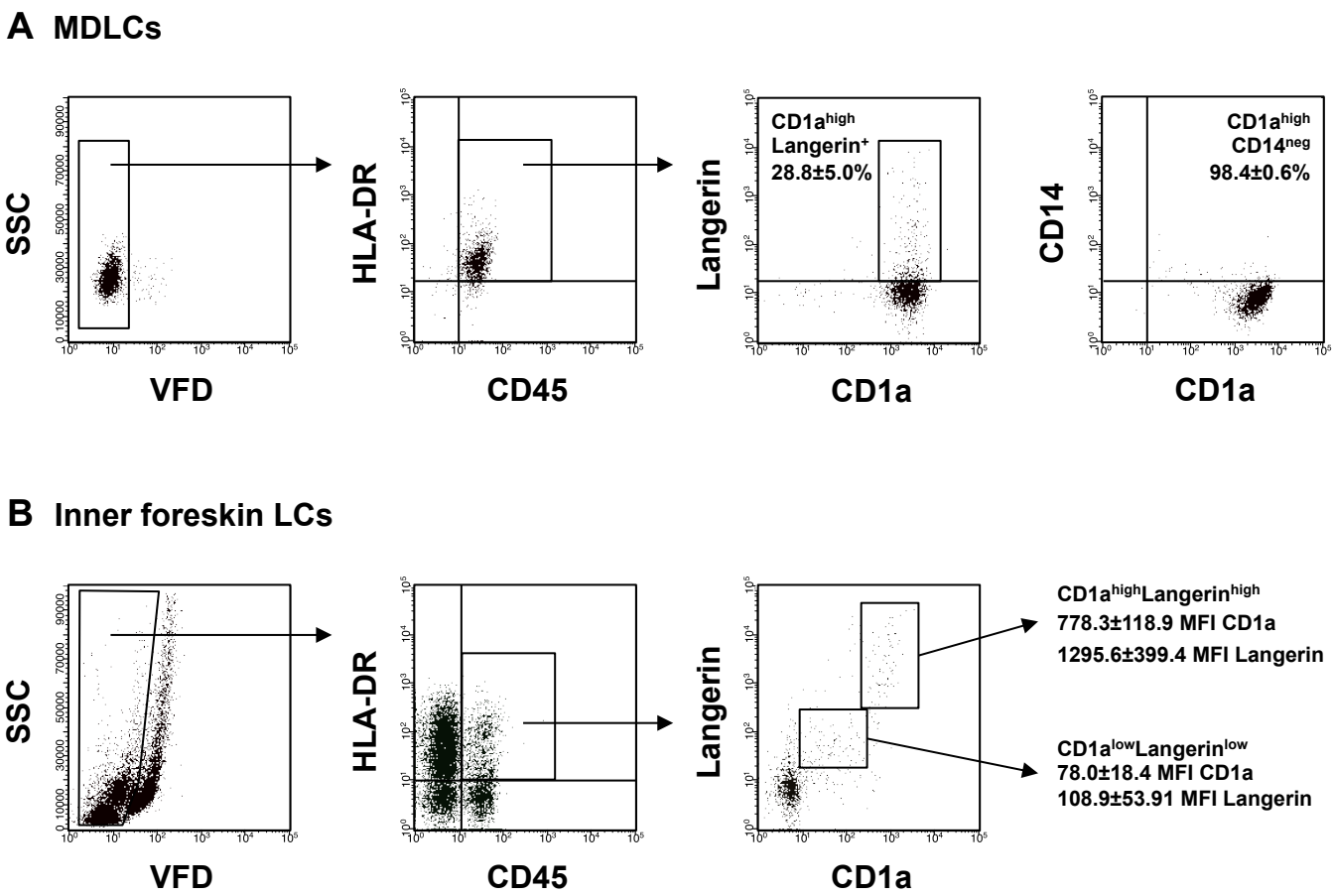

Supplementary Figure 1. Gating strategy and phenotypic characterization of MDLCs and inner foreskin LCs. (A) MDLCs were labeled with Viobility Fixable Dye (VFD), stained for surface expression of CD45, HLA-DR, CD1a, langerin and CD14, and examined by flow cytometry. Shown are representative dot plots, with numbers representing mean±SEM (derived from n=6-10 experiments, using MDLCs prepared from different donors) percentages of double-positive cells, gated on $VFD^{-}CD45^{+}HLADR^{+}$ cells. **(B)** Inner foreskin epidermal cell suspensions were prepared using dispase, followed by trypsin or collagenase enzymatic digestion. The cells were next stained and examined by flow cytometry as above. LCs were separated into $CD1a^{high}Langerin^{high}$ and $CD1a^{low}Langerin^{Low}$ subsets. Shown are representative dot plots, with numbers representing mean±SEM (derived from n=6 tissues, prepared with trypsin or collagenase (n=3 for each)) MFIs, gated on $VFD^{-}CD45^{+}HLADR^{+}$ cells.

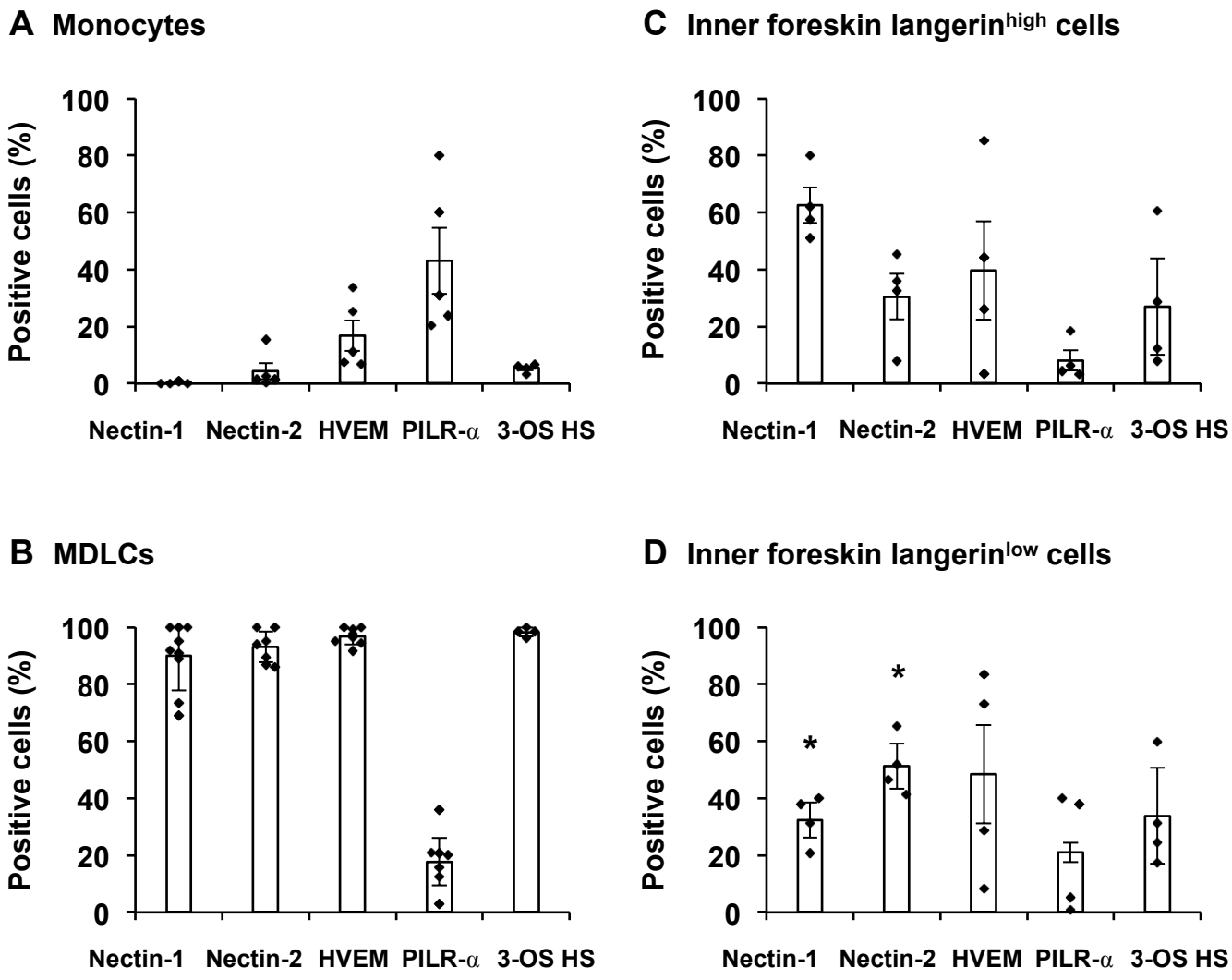

Supplementary Figure 2. Variability of HSV-1 and HSV-2 entry receptors expression. Monocytes **(A)**, MDLCs **(B)** or inner foreskin epidermal cell suspensions **(C, D)**, were labeled for cell-surface expression of HSV entry receptors and langerin, and examined by flow cytometry. Shown are mean±SEM (bars) percentages of positive cells, out of total cells (A), gated on langerin^{+} cells (B) or langerin^{high} (C) / langerin^{low} (D) cells. Each symbol represents a distinct experiment using cells prepared from a different donor. *p=0.0341 for nectin-1 and *p=0.0181 for nectin-2, Langerin^{low} vs. langerin^{high}, paired Student's t-test.

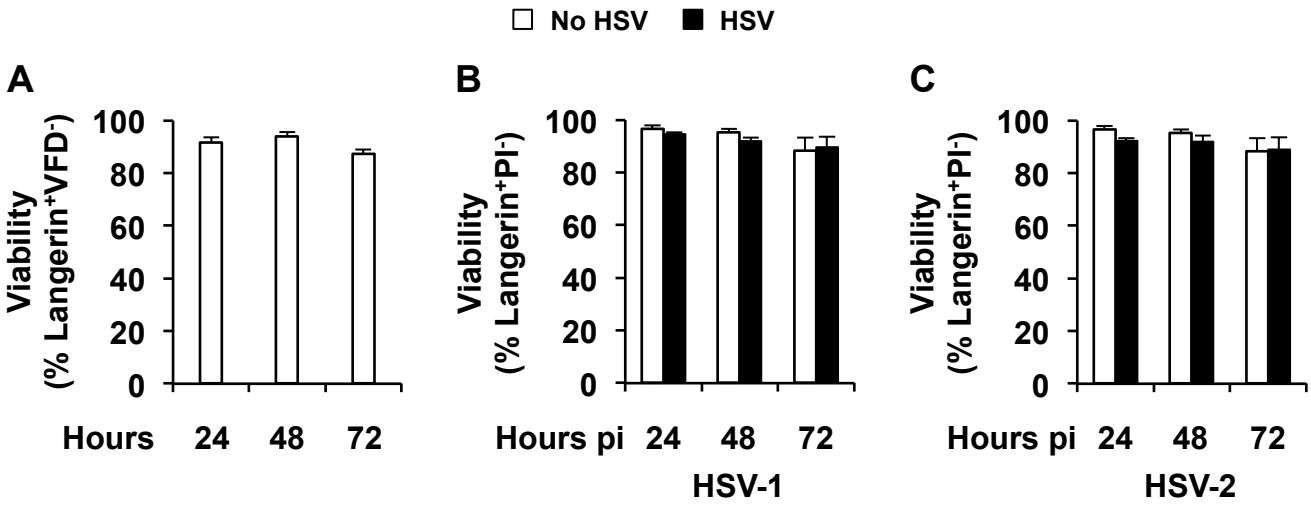

Supplementary Figure 3. Cell viability of MDLCs. MDLCs were left untreated or pulsed for 2hr with HSV-1 (primary isolate 3, MOI=1.0) or HSV-2 (primary isolates 6/7, MOI=0.5). Cells were labeled at the indicated time points with Viobility Fixable Dye (VFD, A) or Propidium Iodide (PI, B and C), followed by langerin surface staining, and evaluated by flow cytometry. Shown are mean±SEM (derived from n=3 (A) and n=7 (B, C) independent experiments using MDLCs from different donors) percentages of viable MDLCs, calculated as ([langerin$^+$VFD$^-$ MDLCs] / [total langerin$^+$ MDLCs] x 100) or ([langerin$^+$PI$^-$ MDLCs] / [total langerin$^+$ MDLCs] x 100).

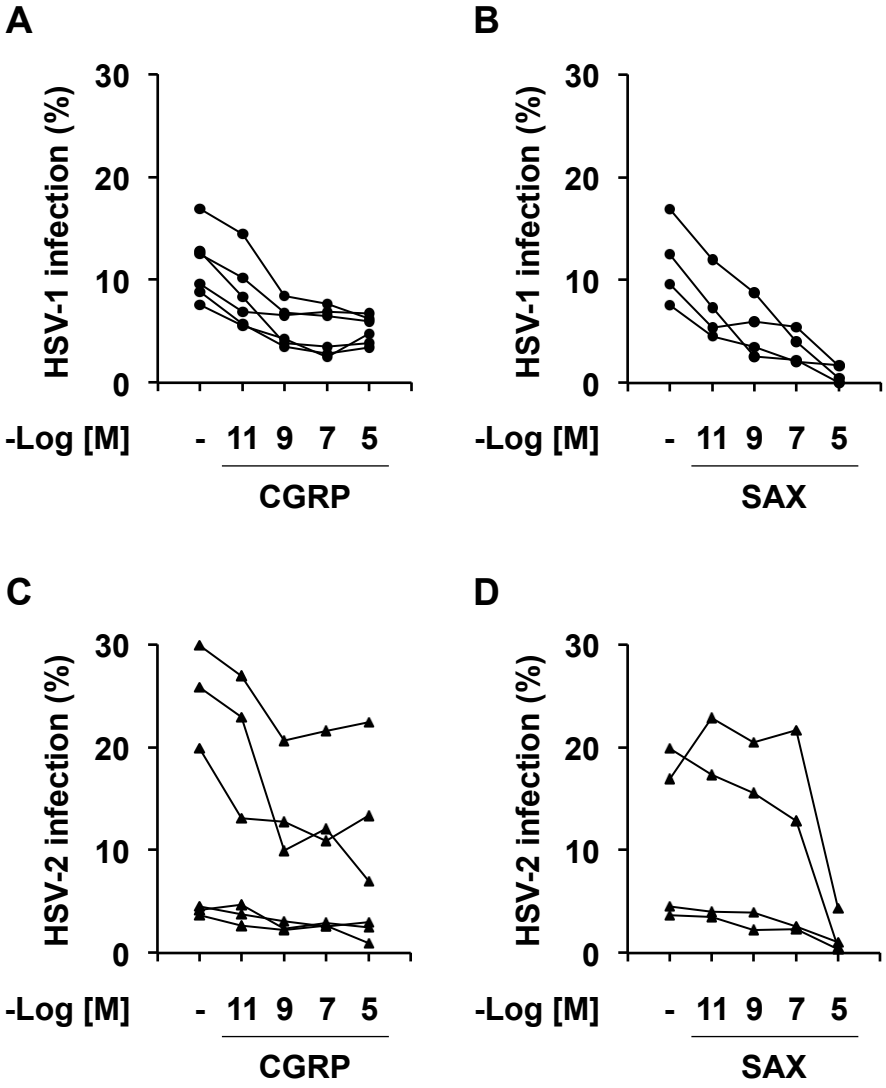

Supplementary Figure 4. CGRP and SAX inhibit human MDLCs infection with HSV-1 and HSV-2. MDLCs were left untreated or pre-treated for 24hr with CGRP or SAX at the indicated molar concentrations. Cells were then pulsed for 2hr with HSV-1 (**A, B**; primary isolate 2 at MOI=0.2 and primary isolate 3 at MOIs=1.0) or HSV-2 (**C, D**; primary isolates 6 and 7 at MOI=0.5), and infection was examined 24hr pi by flow cytometry. Dots (for HSV-1) or triangles (for HSV-2) represent mean percentages of infection (of duplicates), calculated as ([langerin$^+$HSV-1/2-gD$^+$ MDLCs] / [total langerin$^+$ MDLCs] x 100). Each line denotes a different dose response curve obtained using MDLCs from a different individual.

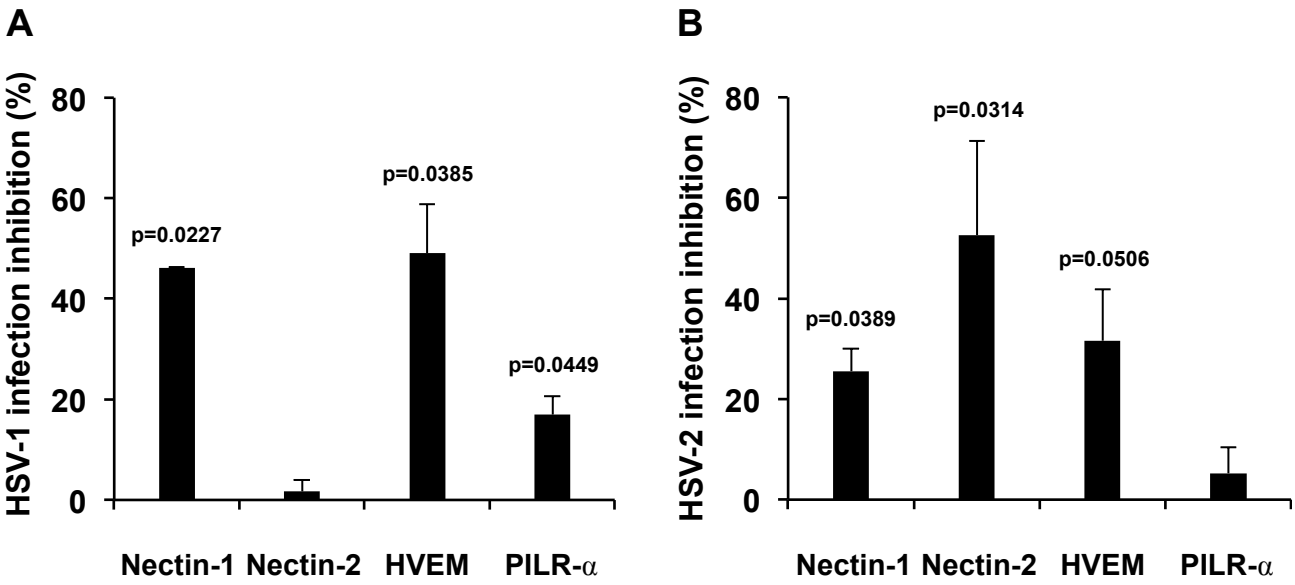

Supplementary Figure 5. Neutralization of HSV-1/2 entry receptors in Vero cells. Confluent monolayers of Vero cells were pre-incubated for 1hr at 37°C with 50μg/mL of nAbs to nectin-1, nectin-2, HVEM and PILR-α vs. non-neutralizing control Abs. The cells were then pulsed with 100pfu of HSV-1 or HSV-2 primary isolates for 2hr and overlaid with immobilization medium. After 3 days, cells were fixed, stained and plaques were counted. Graphs show mean±SEM percentages of inhibition of HSV-1 **(A)** and HSV-2 **(B)** infection, with p-values calculated against control Abs using two-tailed Student's t-test. As expected, nAbs to PILR-α and nectin-2 were subtype specific, while that to nectin-1 and HVEM inhibited infection with both HSV subtypes.

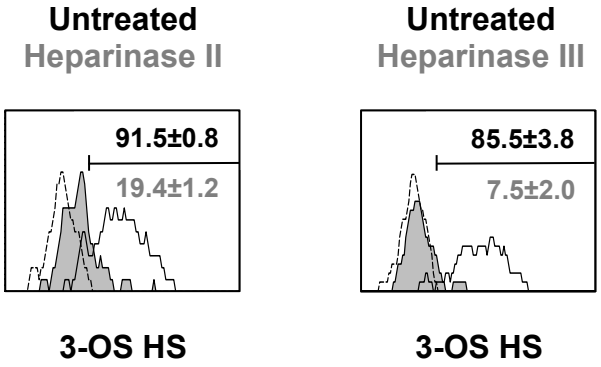

Supplementary Figure 6. Heparinase treatment of MDLCs cleaves surface 3-OS HS. MDLCs were left untreated or pre-incubated for 1hr at 37°C with heparinase II (left panel) or heparinase III (right panel). The cells were next labeled for cell-surface expression of 3-OS HS and langerin and examined by flow cytometry. Representative flow cytometry overlays show 3-OS HS expression in untreated (empty histograms) and heparinase-treated (filled grey histograms) MDLCs vs. isotype controls (broken lines). Numbers represent mean±SEM (of total n=4 donors tested) percentages of positive cells gated on langerin+ cells.

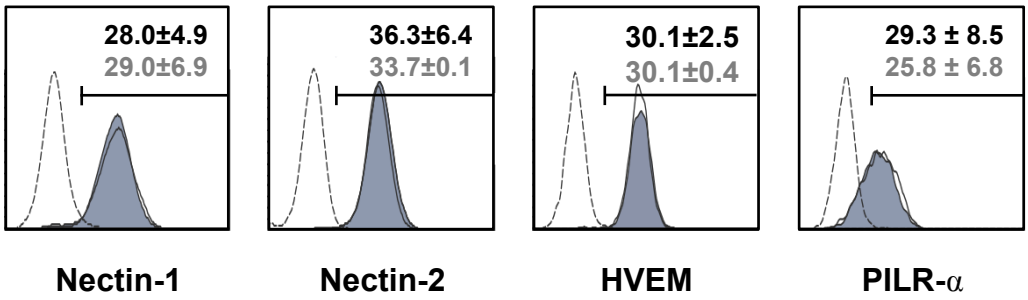

Supplementary Figure 7. CGRP does not affect surface expression of several HSV-1/2 entry receptors. MDLCs were left untreated or pre-treated for 24hr with 100nM CGRP. The cells were next labeled for cell-surface expression of HSV-1/2 entry receptors and langerin. Representative flow cytometry overlays show expression of nectin-1, nectin-2, HVEM and PILR-α in untreated (empty histograms) and CGRP-treated (filled grey histograms) MDLCs vs. isotype controls (broken lines). Numbers (black for untreated, grey for CGRP-treated) represent mean±SEM (n=3) MFIs of each receptor expression, gated on langerin$^+$ MDLCs.

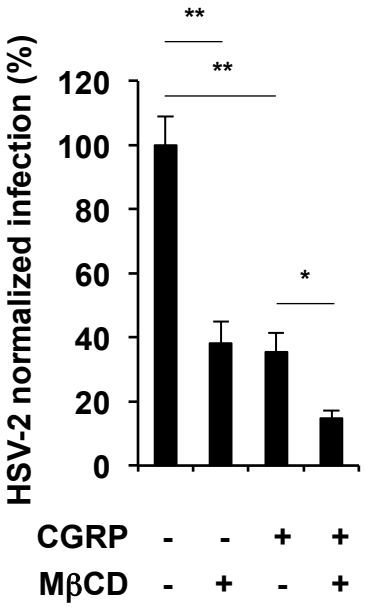

Supplementary Figure 8. HSV-2 infection of MDLCs is cholesterol-dependent. Untreated or CGRP-treated MDLCs were pulsed with HSV-2 (isolate 7 at MOI=0.5), alone or in the presence of methyl beta cyclodextrin (MβCD) as indicated, and infection was measured 24hr pi by flow cytometry. Results represent mean±SEM (n=3) normalized percentages of HSV-2 infection. *p<0.0500, **p<0.0050; two-tailed Student's t-test.

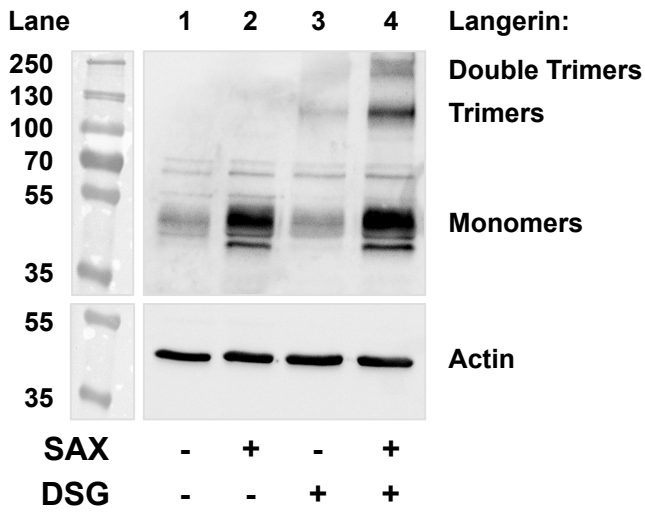

Supplementary Figure 9. SAX induces atypical langerin double trimers. MDLCs, prepared from two additional donors, were left untreated or pre-treated for 24hr with 1μM SAX. Shown is a representative Western blot of langerin expression in untreated (lane 1), SAX-treated (lane 2), untreated / DSG cross-linked (lane 3) and SAX-treated / DSG cross-linked (lane 4) MDLCs. Langerin appears as ~47kDa monomers, ~120kDa trimers and ~240 double trimers.

Supplementary Table 1: List of Abs used in the current study

Antibody	Clone	Dilution / Conc.	Source
Abs for phenotypic analysis of MDLCs and inner foreskin epidermal cells			
PO-conjugated mouse-anti-human CD45	HI30	1:100	Invitrogen
APC-H7-conjugated mouse-anti-human HLD-DR	G46-6	1:100	BD Pharmingen
APC or PE-conjugated recombinant human-anti-human langerin	REA770	1:100	Miltenyi Biotec
APC or PE-conjugated mouse-anti-human CD1a	HI149	1:10	BD Pharmingen
FITC-conjugated mouse-anti-human CD14	RMO52	1:10	Beckman Coulter
Abs for expression of HSV-1/2 entry receptors			
APC-conjugated, mouse-anti-human nectin-2	R2.477	1µg/ml	Thermo Fischer
APC-conjugated mouse-anti-human HVEM	9G11	1µg/ml	R&D Systems
Non-conjugated mouse-anti-human nectin-1	R1.302	1µg/ml	Novus
Non-conjugated rabbit-anti-human PILR-α	2175B	1µg/ml	R&D Systems
VSV-tagged scFv against human 3-O HS	HS4C3	1:10	[1]
Mouse anti-VSV tag	P5D4	1:1500	Sigma
Cy5-conjugated goat anti-mouse IgG1		1:200	Southern Biotech
Cy5-conjugated donkey anti-rabbit IgG		1:200	Jackson
PE-conjugated mouse-anti-human langerin	DCGM4	1:10	Beckman Coulter
Neutralizing Abs			
Mouse-anti-human nectin-1	R1.302	50µg/ml	[2] Novus
Mouse-anti-human nectin-2	R2.525	50µg/ml	[3] Biorad
Rabbit-anti-human PILR-α	2175B	50µg/ml	R&D Systems
Rabbit-anti-human HVEM [a]		50µg/ml	
Mouse-anti-human langerin	817G7	50µg/ml	Dendritics
Abs for HSV-1/2 infection			
PE-conjugated mouse-anti-human langerin	DCGM4	1:10	Beckman Coulter
APC or PE-conjugated recombinant human-anti-human langerin	REA770	1:100	Miltenyi Biotec
FITC-conjugated mouse-anti-HSV-1/2-gD	M86670F	5µg/ml	Fitzgerald

Abbreviations: APC, Allophycocyanin; Cy5, Cyanin-5; FITC, Fluorescein isothiocyanate; PO, Pacific orange; PE, Phycoerythrin.

[a] Kind gift from Dr. Gary H. Cohen, University of Pennsylvania, USA [4].

References

1. Ten Dam GB, Kurup S, van de Westerlo EM, Versteeg EM, Lindahl U, Spillmann D *et al.* 3-O-sulfated oligosaccharide structures are recognized by anti-heparan sulfate antibody HS4C3. *J Biol Chem* 2006; **281**(8)**:** 4654-4662.
2. Tiwari V, Oh MJ, Kovacs M, Shukla SY, Valyi-Nagy T, Shukla D. Role for nectin-1 in herpes simplex virus 1 entry and spread in human retinal pigment epithelial cells. *FEBS J* 2008; **275**(21)**:** 5272-5285.
3. Lopez M, Cocchi F, Menotti L, Avitabile E, Dubreuil P, Campadelli-Fiume G. Nectin2alpha (PRR2alpha or HveB) and nectin2delta are low-efficiency mediators for entry of herpes simplex virus mutants carrying the Leu25Pro substitution in glycoprotein D. *J Virol* 2000; **74**(3)**:** 1267-1274.
4. Connolly SA, Landsburg DJ, Carfi A, Wiley DC, Eisenberg RJ, Cohen GH. Structure-based analysis of the herpes simplex virus glycoprotein D binding site present on herpesvirus entry mediator HveA (HVEM). *J Virol* 2002; **76**(21)**:** 10894-10904.